

Received May 5, 2021, accepted May 12, 2021, date of publication May 17, 2021, date of current version June 2, 2021.

Digital Object Identifier 10.1109/ACCESS.2021.3080704

A Quasi-Oppositional Method for Output Tracking Control by Swarm-Based MPID Controller on AC/HVDC Interconnected Systems With Virtual Inertia Emulation

IMAN M. HOSEINI NAVEH¹, ELYAS RAKHSHANI², (Senior Member, IEEE),
HASAN MEHRJERDI³, (Senior Member, IEEE),
AND MOHAMED A. ELSAHARTY⁴, (Member, IEEE)

¹Department of Electrical Engineering, Gonabad Branch, Islamic Azad University, Gonabad 9691664791, Iran

²Department of Electrical Sustainable Energy, Delft University of Technology, 2628 CD Delft, The Netherlands

³Department of Electrical Engineering, Qatar University, Doha, Qatar


⁴Research Institute for Autonomous Systems, University of North Dakota, Grand Forks, ND 58202, USA

Corresponding author: Elyas Rakhshani (rakhshani@ieee.org)

This work was supported by the Qatar National Library.

ABSTRACT This paper presents a comprehensive evaluation of the effect of quasi oppositional - based learning method utilization in output tracking control through a swarm-based multivariable Proportional-Integral-Derivative (SMPID) controller, which is tuned by a novel performance index based on the step response characteristics in multi-input multi-output (MIMO) system. The role of the proposed quasi oppositional based SMPID controller is to modify the tracking strategy on AC/HVDC interconnected systems while reducing the related cost function. The proposed analysis is established considering the most highly cited, well-known tested and newly expanded swarm-based optimization algorithms (SBOAs), such as Grasshopper Optimization Algorithm (GOA), Grey Wolf Optimization (GWO), Artificial Fish Swarm Algorithm (AFSA), Artificial Bee Colony (ABC) and Particle Swarm Optimization (PSO). These methods are used in the tuning process of multivariable PID (MPID) controller for output tracking control of an interconnected AC/DC system with virtual inertia emulation-based HVDC capabilities. The virtual inertia-based HVDC model, which is using a derivative technique, is attached for enhancing the system frequency dynamics with fast power injection during the contingency. The potential possibility for achieving a suitable assessment about the velocity reaction, the flexibility response, and the accuracy of the tracking process is provided by four different scenarios which are operated by step load changes as essential inputs in AC/HVDC interconnected MIMO system. Also the proposed fitness function, as deviation characteristics of the step response in MIMO transfer function in virtual inertia emulation based HVDC model, is compared with integral time absolute error (ITAE), as the standard performance index in the optimization process. The results are compared with the conventional tuned MPID (C - MPID) controller using MATLAB software. The obtained analysis emphasizes how the tuned SMPID can significantly increase the capability of tracking control on the proposed AC/HVDC interconnected model.

INDEX TERMS Frequency control, virtual inertia, quasi oppositional-based learning method (QO-BL), grey wolf optimization (GWO) algorithm, grasshopper algorithm (GOA), artificial fish swarm algorithm (AFSA), artificial bee colony (ABC), particle swarm optimization (PSO), quasi oppositional-based GWO (QO-GWO), quasi oppositional-based GOA (QO-GOA), quasi oppositional-based AFSA (QO-AFSA), quasi oppositional-based PSO (QO-PSO), multivariable proportional-integral-derivative (MPID) controller, conventional tuned MPID (C-MPID), swarm-based MPID controller (SMPID), swarm-based optimization algorithms (SBOAs), AC/HVDC interconnected system with energy storage systems (AC/HVDC with ESS).

The associate editor coordinating the review of this manuscript and approving it for publication was Huiling Chen .

I. INTRODUCTION

The comprehensive growth and rapid development of AC systems into a multi-area interconnected scenario, including the increasing level of high power converter applications in modern power systems, is giving rise to a very multiplex and challenging issue, which will affect the overall power system and particularly the frequency control in AC/DC systems [1]. AGC of a multi-area power system during load and resource variation is a principal mechanism that can simplify different targets such as frequency restoration, tie-line power flow control between authority areas, and economic dispatch of generation units [2], [3]. Multi-area interconnections can be prepared by AC or DC tie-lines enabling the scheduled power exchange between different control areas and also supplying adequate support in case of abnormal conditions. Because of several limitations associated with AC lines, especially for long-distance connections, HVDC links have obtained rising attention over the last years. HVDC interconnection is one of the important applications of power converters in multi-area interconnected power systems, which could drive useful advantages like fast and bidirectional controllability, POD, and frequency stability support [4], [5]. Thus, in some parts of the world, HVDC or hybrid interconnections, including parallel AC and DC interconnections enhanced earlier the preferred solution [6], [7]. Newly, for rising the dynamic performance of AC/DC systems, various attempts have been accomplished to make grid-connected converters act like synchronous generators, by supplying more inertia to the system [8]. One of the recent concepts in this topic is related to the virtual inertia emulation task. This virtual inertia is emulated by using modern control of power converters by attention to the added short-term energy storage system (ESS) within the DC link of the HVDC converters [9]. It can increase the possibility of having a higher amount of distributed generation systems, connected to the grid through power converters, without hindering the system stability.

Since the concept of virtual inertia in AC/DC interconnected power systems is relatively new, there is a need to extend more research on advanced control methodologies for such multi-input multi-output (MIMO) systems.

By attention to the obtained experiences, especially in MIMO physical systems, MPID controller has the most efficient performance among other kinds of controllers [10]. Simplified, functional, and utilized performance are the main reasons for using MPID controller more than others [11]–[15]. However, Ho *et al.* [16] explained that only 20% of PID control loops are in suitable conditions. The others are not, where 30% of PID controllers are not able to achieve well due to the absence of setting parameters, 30% due to the installation of a controller system operating manual, and 20% due to the use of default controller parameters. Recently, the MPI controllers design has been noticed for different processes such as Industrial Scale - Polymerization Reactor [17], Coupled Pilot Plant Distillation Column [18], Narmada Main Canal [19], Quadruple-Tank Process [20], Boiler-Turbine Unit [21], and Wood-Berry

Distillation Column [22]. Kumar *et al.* [17] had presented a combination method based on the approximation of relative gain array (RGA) concept to the multivariable process.

As we know, in most of the applied industrial systems, the main targets of the control system design are the stabilization proper tracking of the reference signal for a closed-loop system. For the case of stabilization, power system stabilizers (PSS) are clear examples that can mitigate the oscillations, caused by disturbances [23]–[26]. In roll stabilized missiles, which are called no-roll missiles, a part of missile autopilot as a control system is responsible for mitigating the rolling oscillations [27]. Also in the invertible pendulum, the principal aim of the controller design is stability maintenance around the vertical equilibrium point. All described above cases are good samples for regulator or stabilizer systems. In these cases, all reference inputs are zero, ($r(t) = 0$), and this will be the most important part of the system's design for such application. In many other applied systems, in addition to stabilizing, the other main aim will be signal tracking as well [28]–[30]. In these cases, unlike regulator systems, all reference inputs are non-zero ($r(t) \neq 0$), and therefore in tracking control, the closed-loop outputs will follow the reference inputs. So they are called a tracker. For this case, electrical machines are suitable samples, which their speed should follow the desired value [31]–[33].

By attention to the above-explained cases, it can be concluded that the main motivation of control of a dynamic system is to pressurize the plant to perform enough closely to (to track accurately) its eligible output treatment over some, usually pre-specified, time interval and under real (usually unpredictable and unknown) both external (input) actions and initial conditions [34]. Therefore, it is obvious that the principal goal of control is to satisfy that the dynamic model of plant displays the desired kind of output tracking. These goals can be easily satisfied by the proper design of the swarm based-MPID controller, which is part of the controller design in this paper.

In the following work, the Quasi - Oppositional (QO) based learning, as a novel applied approach for achieving accurate and suitable output tracking control, is integrated into the high impact, well satisfied, and freshly developed swarm-based optimization algorithms (SBOAs). Recently, QO - BL technique is utilized to solve power system problems, including hydropower system operation [35], stability analysis of hybrid power system [36], load frequency control [37], automatic generation control [38]–[40], optimal allocation power devices [41], [42] and economic load dispatch problem [43]. Also, some developments are achieved on this method to modify its performance in the problem-solving process [44]. Some of the enhanced optimization researchers about the proposed SBOAs in this paper are such as Grasshopper Optimization Algorithm (GOA) [45], Grey Wolf Optimization (GWO) algorithm [46], Artificial Fish Swarm Algorithm (AFSA) [47], Artificial Bee Colony (ABC) [48] and Particle Swarm Optimization (PSO) [49]. According to the above applications,

the proposed QO - BL method is applied for tuning Swarm-based MPID (SMPID) controller, in output tracking control of an interconnected AC/HVDC system with ESS model. This study is the first of its kind which can enhance the overall virtual inertia-based AC/DC interconnected system through an accurate and exact output tracking control approach.

The contributions of this paper are reflected through the following aspects:

- (i) To the best of the author's knowledge, not too many research works have been reported for designing an advanced higher-level control for suppressing the overall performance of such a multivariable AC/DC system with virtual inertia-based HVDC functionalities.
- (ii) To fill this gap, the research conducted in this paper is focused on a novel advanced control design for the derivative-based inertia emulation concept through the converter stations of the HVDC link. The designed high-level control is achieved by using an advanced SMPID controller in a multi-machine AGC system.
- (iii) The incorporation of swarm-based techniques with MPID control is leading to an accurate hybrid solution that can be used as an evaluated strategy for the output tracking problem of ESS-based virtual inertia emulation AC/DC systems.
- (iv) The main part of optimization in this work is focused on a proposed performance index as a function including the linear combination of step response features such as stability index (SI) and settling time (ST) and rise time (RT). Finding the best MPID coefficients, as the main target among this process, is realized using the minimization of the proposed performance index. Two different applications from this proposed performance index, are achieved through the authors on MPI controller [50], [51]. The optimization process is achieved by the extraction of step response features from the transfer function matrices in the AC/HVDC model. For achieving a better comparison for the proposed SMPID performance, at first typical MPID controller is tuned using a conventional approach and then the designed SMPID controllers are differentiated versus the conventional type.
- (v) An innovative optimization method is presented by employing QO - BL method with SBOAs.
- (vi) Furthermore, a comprehensive assessment is presented for demonstrating the performance of the optimal tuning method, for achieving the best MPID's coefficients, through swarm-based algorithms. The presented swarm-based methods are GWO, GOA, AFSA, PSO, and ABC because of their advantages over other algorithms. Some of the main advantages are as follows:

- 1) convenience of implementation due to their simple structure.
- 2) less storage and computational requirements.
- 3) faster convergence due to the continuous reduction of search space.
- 4) fewer decision variables and therefore their ability in avoiding local minima.
- 5) presentation of better stability and robustness.

The rest of the present work is arranged as follows: The dynamic model of the test system is attended in Section II, followed by the virtual inertia emulation-based AC/HVDC interconnected system. The theory of tracking control and its importance of utilization is reviewed in Section III, followed by the output tracking control strategy. A brief outline of SBOAs is developed in Section IV, tracked by the swarm-based optimization algorithms. Also, the concept of the QO method is presented in Section V as the QO - BL method. The simulation results, as the last Section is considered for the performance characteristics evaluation, including the tracking flexibility, robustness, and sensitivity.

II. VIRTUAL INERTIA-BASED AC/HVDC SYSTEM

This section is focused on the presentation of a definition for the concept of inertia emulation on AC/HVDC interconnected systems as a two-area model.

A. DYNAMIC MODEL

As we know, AGC as a higher-level control strategy produces the set-points for all the local components which are under control by their local controllers and also inertia emulation by a derivative term control strategy suitable for Power Oscillation Damping (POD) and frequency support applications in large-scale AGC interconnected power systems. In this paper, the proposed model consists of parallel AC and HVDC lines and energy storage systems (ESS) with a scheme of a two-area AC/DC power system. Inertia emulation is known as a capable method to utilize the derivation of the system frequency proportionally to modify the active power reference of a converter. Then the emulated inertia can lead to moderate the performance of the system dynamics on the inertia response. This concept is the derivative control which calculates the rate of change of frequency (ROCOF), and can be described as:

$$\Delta P_{emulate} = k_a \omega_0 \frac{d}{dt} \Delta \omega \quad (1)$$

where $\Delta P_{emulate}$ is the power reference and ω_0 is the nominal frequency and k_a the inertial proportional conversion gain which can be chosen basis on a renewing tuning process for optimizing the frequency deviations. The block diagram of a two-area system with parallel AC/HVDC links and added ESS for providing virtual inertia emulation is performed in Figure 1.

As it is mentioned in Fig. 1, for achieving the performance improvement of ESS models, two converters are considered

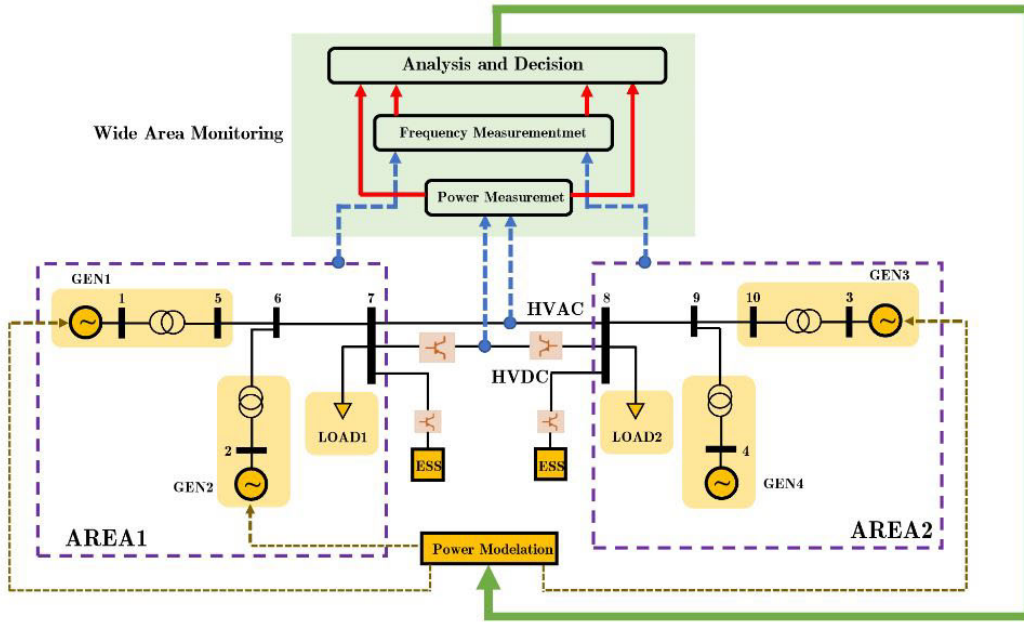


FIGURE 1. Block diagram of the studied AC/HVDC with ESS model.

in accordance with HVDC coordination and secondary frequency control signals to minimize the deviations of system frequency during contingencies. The large-area frequency and AC/DC power flow measurements are converged in each area and tie-line and sent to the control center via communication networks for the HVDC coordination and secondary frequency control operation. It is important that instead of these external signals, the virtual inertial emulation is utilizing the local information only, which implies a faster response [52], [53].

Also, Fig. 2, describes the frequency dynamics model of the two-area AC/DC interconnected system with ESS for inertia emulation [54]. As it is observed, the frequency deviation of Area i in the Laplace domain can be expressed as:

$$\Delta\omega_i = \frac{K_{pi}}{1 + sT_{pi}} [\Delta P_{mi} - \Delta P_{li} - (\Delta P_{tieACi} + \Delta P_{DC} + \Delta P_{ESSi})] \quad (2)$$

where ΔP_{mi} and ΔP_{ESSi} denote total active power from all generation units (GENs) within Area i and k and the power variation for emulating inertia, respectively.

AC power flow deviations ΔP_{tieACi} of these two areas. K_{pi} and T_{pi} are calculated as the model gain and time constant, respectively. Also the step load changes in area i is mentioned as ΔP_{li} . The power deviation from ESS in each area, ΔP_{ESSi} , can be calculated as:

$$\Delta P_{ESSi} = \frac{J_{emi}}{1 + sT_{ESSi}} (\Delta\omega_i) \quad (3)$$

It is so noticeable that practically the virtual inertia emulation model can be tender to the input noises. Therefore, it is possible to utilize a low pass filter which can be collected to the proposed model for moderating the effects of

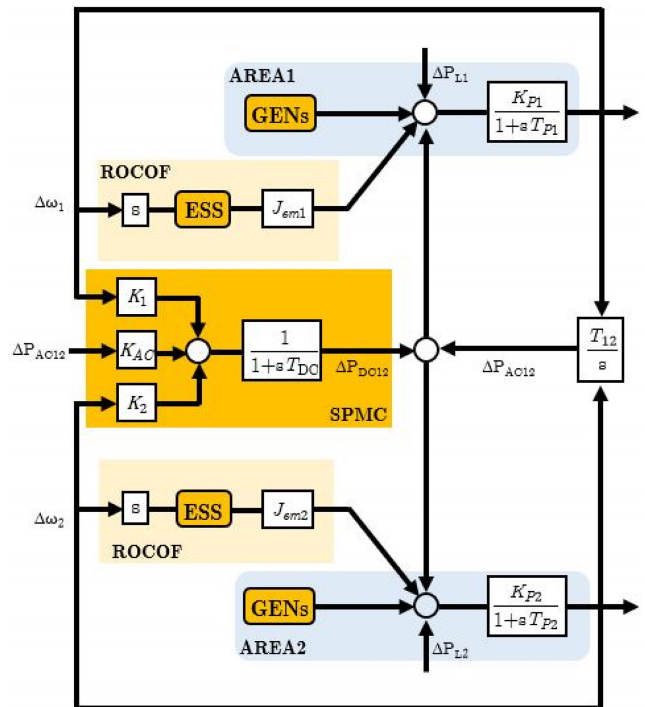


FIGURE 2. Two-area AC/HVDC system with ESS model.

noises. To consider this concept, the dynamics of such a filter with storage elements are added by the time constant T_{ESSi} . Therefore this constant parameter is collected for imitating the control dynamic characteristic of the storage devices and the new area control error of i^{th} area will be obtained as:

$$ACE_i = \beta_i \Delta\omega_i + [\Delta P_{tieACi} + \Delta P_{DC}] \quad (4)$$

where for Area i , β_i is the frequency bias. Also, we can calculate the other main state variables as:

$$\Delta P_{tieACik} = \frac{T_{i,j}}{s} [\Delta \omega_i - \Delta \omega_k] \quad (5)$$

$$\Delta P_{DCref} = K_i \Delta \omega_i + K_k \Delta \omega_k + K_{AC} \Delta P_{tieAC,ik} \quad (6)$$

$$\Delta P_{DCik} = \frac{1}{1 + sT_{DC}} \Delta P_{DCref} \quad (7)$$

where ΔP_{DCref} is the desired DC power reference for the HVDC line and the time constant for the DC link is called T_{DC} . Also K_i , K_k and K_{AC} are the proportional coefficients for the frequency deviations $\Delta \omega_i$, $\Delta \omega_k$ and AC power flow deviations $\Delta P_{tieAC,ik}$ of these two areas, respectively.

B. MATHEMATICAL AC/HVDC MODEL WITH ESS STRATEGY

As mentioned in the previous section, we can have a total MIMO linearized mathematical steady-state model of the two-area AC/DC interconnected power system with virtual inertia emulation strategy:

$$\begin{cases} \Delta \dot{x}_{ESS}(t) = A_{(12 \times 12)}^{ESS} \Delta x_{ESS}(t) + B_{(12 \times 2)}^{ESS} \Delta u_{ESS}(t) \\ \Delta y_{ESS}(t) = C_{(2 \times 12)}^{ESS} \Delta x_{ESS}(t) \end{cases} \quad (8)$$

$$\Delta x_{ESS} = \begin{bmatrix} \Delta \omega_1 & \Delta \omega_2 & \Delta P_{m1} & \Delta P_{m2} & \Delta P_{m3} & \Delta P_{m4} \\ \Delta ACE_1 & \Delta ACE_2 & \Delta P_{tieAC12} & \Delta P_{DC} & \Delta P_{ESS1} & \Delta P_{ESS2} \end{bmatrix}^T \quad (9)$$

$$\Delta u_{ESS} = [\Delta P_{11} \quad \Delta P_{12}]^T \quad (10)$$

$$\Delta y_{ESS} = [\Delta \omega_1 \quad \Delta \omega_2]^T \quad (11)$$

All of the main coefficients and constant values are available in [54]. As it was shown in Figures 1 and 2, it is supposed that there is a parallel AC/HVDC link between Area i and Area k , where both converter stations of the HVDC link are simplified using ESS concepts. By attention to the dynamic of the virtual inertia emulation model, the main equations of these two AC/HVDC interconnected areas in the Laplace domain will be as follows (2) – (7).

By considering the proposed method, a transfer function matrix using 2 inputs and 2 outputs is designed by (12). In all strategies, $\Delta \omega_1$ and $\Delta \omega_2$ are output variables:

$$\begin{bmatrix} \Delta \Omega_1^{ESS}(s) \\ \Delta \Omega_2^{ESS}(s) \end{bmatrix} = \begin{bmatrix} G_{11}^{ESS}(s) & G_{12}^{ESS}(s) \\ G_{21}^{ESS}(s) & G_{22}^{ESS}(s) \end{bmatrix} \begin{bmatrix} \Delta U_1^{ESS}(s) \\ \Delta U_2^{ESS}(s) \end{bmatrix} \quad (12)$$

$$G_{Tf}^{ESS}(s) = \begin{bmatrix} G_{11}^{ESS}(s) & G_{12}^{ESS}(s) \\ G_{21}^{ESS}(s) & G_{22}^{ESS}(s) \end{bmatrix} \quad (13)$$

Figure. 3 denotes the block diagram model for the presentation of (12) and (13), as the MIMO transfer function model.

III. OUTPUT TRACKING CONTROL STRATEGY

It seems that the servomechanism or servo-system theory is historically considered as the first study about the concepts of tracking control. The main reason for this calling is that the applied controller should force the plant output to follow

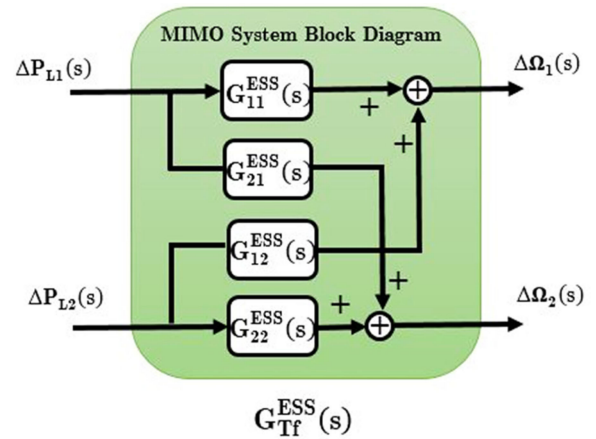


FIGURE 3. MIMO transfer function model for AC/HVDC with ESS.

the time-varying desired output [55]. On the other hand, output tracking, as the trajectory flatness-based tracking problem [56], [57], means that the main model is controlled in a way that its output follows a desired reference trajectory.

Assume a linear multivariable plant, as shown in Figure 4. As it is considered, an exogenous system causes a reference signal (w), and subsequently, it is our target to track desired reference signal by generated output such a way that the error signal between them tends to zero. Also, a controller is designed by measuring the signal y . We design a controller with measurement signal y .

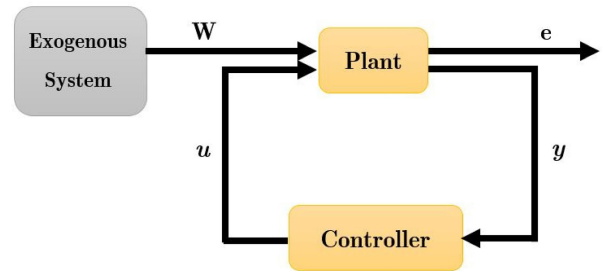


FIGURE 4. Configuration of output tracking control strategy.

By attention to Figure 4, the dynamic equations of the plant can be written as follows:

$$\begin{cases} \dot{X}_{Plant}(t) = A_{Plant} X_{Plant}(t) + B_{Plant} U_{Plant}(t) + E_W W(t) \\ Y_{Plant}(t) = C_{Plant}^y X_{Plant}(t) + D_{Plant}^{yu} U_{Plant}(t) + D^{yw} W(t) \\ E_{Plant}(t) = C_{Plant}^e X_{Plant}(t) + D_{Plant}^{eu} U_{Plant}(t) + D^{ew} W(t) \end{cases} \quad (14)$$

In the first above equation, $X_{Plant} \in \mathbb{R}^n$ and $U_{Plant} \in \mathbb{R}^m$ are the plant states and inputs, respectively. Also in the exogenous system, $W \in \mathbb{R}^p$ is the state of the model. For the second above equation, $Y_{Plant} \in \mathbb{R}^q$ is the measurement which explains the send data to the controller. And finally, the third equation describes the error, $E_{Plant} \in \mathbb{R}^r$, between the actual controlled plant output and the reference signal.

In addition to the described cases, the exogenous model, as an individual system, which generates both terms of $E_W W(t)$ and $D^{sw} W(t)$, has a state-space realization which its dynamic equation is as follows:

$$\dot{W}_{Plant}(t) = A_{Exosys} W(t) \quad (15)$$

By considering to the state feedback controller equation, $U_{Plant}(t) = -FX_{Plant}(t) + GW(t)$, we have a closed-loop system which follows:

$$\begin{cases} \dot{X}_{Plant}(t) = (A_{Plant} - B_{Plant}F) X_{Plant}(t) \\ \quad + (E_W + B_{Plant}G) W(t) \\ E_{Plant}(t) = (C_{Plant}^e - D_{Plant}^{eu}F) X_{Plant}(t) \\ \quad + (D_{Plant}^{eu} + G) W(t) \end{cases} \quad (16)$$

As it seems, by attention to (16), the main target is to design a kind of controller that achieves both output tracking and internal stability. Internal stability means that if we ignore the exogenous system and set W equal to zero, the closed-loop system, including the plant and the applied controller, is asymptotically stable [58].

By attention to [56] and [57], the flatness-based tracking control will be realized for the controllable systems. Therefore, the proposed AC/HVDC with ESS model in (8), can follow from the output tracking laws because of controllability. In this paper, we are going to find a suitable MPID controller for achieving the most optimized and closed conditions for output tracking control. Therefore a new fitness function is proposed to tune quasi opposite swarm-based MPID (QO-SMPID) through the main characteristics of the step response for the MIMO test model. Also, it is available to assess the performance of the proposed QO-SMPID by comparing the accuracy, flexibility, and reaction velocity of the presented tracker in two different scenarios. Additionally in this work, an individual Section is presented that the other standard index, integral time absolute error (ITAE), is compared with the performance of the applied fitness function.

IV. SWARM – BASED OPTIMIZATION ALGORITHMS

The first and the most typical definition for “swarm” is based on a similar and simple set of agents that are interconnected locally among themselves. So by considering the above explanation, SBOAs have been introduced as a subset of nature-inspired, crowd-based algorithms that can generate low-cost, fast, and robust solutions for an extensive set of multiplex problems [59], [60]. On the other hand, SBOAs can be called an individual branch of artificial intelligence (AI) which are applied to implement the communal behavior of social swarms in nature. The social interconnections between swarm individuals can be either direct or indirect [61].

Simultaneous to introduce swarm-based computational models, there has been a mutation in the number of scientific activities which presented the successful utilization of SBOAs in a various set of optimization tasks and complex problems. SBOAs are known as a subset from a bigger set which are called metaheuristic methods. A metaheuristic

is a high-multiplex problem that presents a set of strategies to expand heuristic optimization algorithms. By attention to the recently obtained experiences in complicated or large problems, metaheuristics are capable to give a suitable trade-off between solution quality and computing time. Figure 5 presents a biology-based classification according to the nature of SBOAs from 1980 to 2017. As it is observed, insect, mammal, bird, fish, bacteria, frog, and group-based hunting are the main taxonomies of SBOAs. In this section, a relevant investigation is performed to find the number of related papers in some of the important scientific databases, such as IEEE Xplore, ScienceDirect, and SpringerLink. For achieving a suitable search string, the authors considered the name of SBOAs and “PID Controller”, as the major keywords, and also they investigated the publication value of relevant papers in selected databases. The obtained results from this research, are utilized in Table 1(a) and (b). Also, these tables are applied to omit superfluous information and introduce SBOAs completely. The main SBOAs framework will be categorized as follows:

- (a) Initialization of the swarm.
- (b) Determination of the stop constraints.
- (c) Calculation of the objective function.
- (d) Upgrade and movement of the search agents.
- (e) Extraction of the global best solution.

Certainly, for SBOAs, the definition of the algorithm parameters is achieved before the initialization stage. The next stage will be done to prevent the performance of SBOA by means of the stop constraints check. The third stage of the SBOA framework is to assess the objective function value which is accountable for the search agents. As was described in stage (b), the values of SBOA parameters should be explained by some standard mathematical functions as the objective function. The search agents in an SBOA will be upgraded and moved according to the typical mathematical structure of its algorithm.

Based on recent researches, the variety of these methods has significantly increased over the last years [62]. Some of the recent optimization algorithms, including monarch butterfly optimization (MBO) [63], elephant herding optimization (EHO) [64], moth search (MS) algorithm [65], Slime mould algorithm (SMA) [66], and Harris hawks optimization (HHO) [67], which, are not deniable in comparison with the applied SBOAs in this work. By considering the obtained results from the tables, the authors decided to investigate some of the high applicability, well-satisfied tested and freshly developed methods among SBOAs, such as Grasshoppers Algorithm (GOA), Grey Wolf Optimization (GWO), Artificial Fish Swarm Algorithm (AFSA) and Artificial Bee Colony (ABC) and Particle Swarm Optimization (PSO), for utilizing as the main SBOAs in the quasi oppositional process. As it is considered in these tables, some of the columns in this academic online investigation are specified using a solid line. This kind of mark in the tables emphasizes to be inadequate the number of published relevant researches in the corresponded database. There are

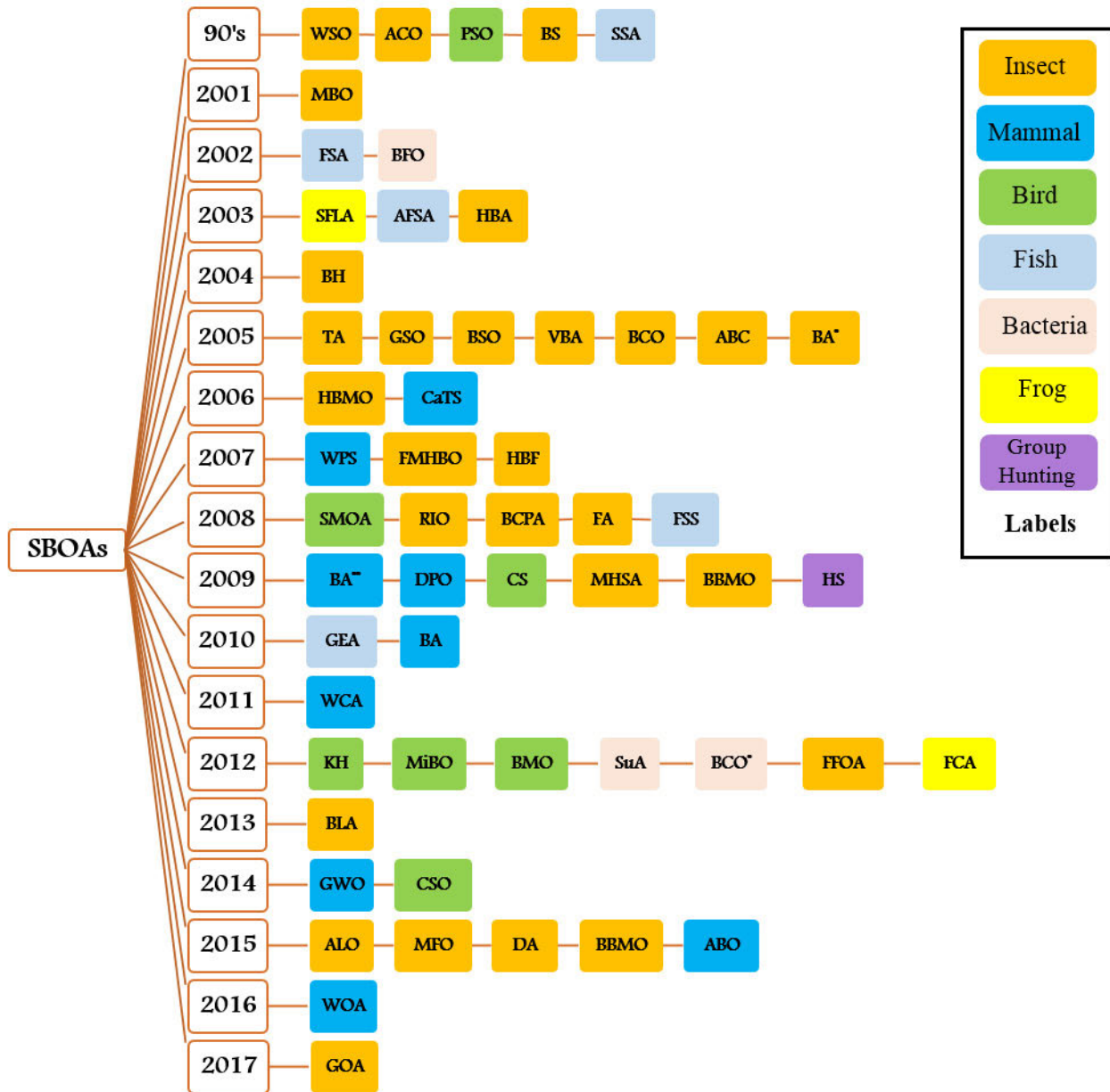


FIGURE 5. Biology – Based Classification of Swarm-Based Optimization Algorithms (SBOAs).

some reasons for arising this case in the tables such as (i) some of these described SBOAs, were developed in the next years and therefore new well-evaluated versions were created from primary previous algorithms which the investigators were tended to simulate their optimization problems with the newer similar SBOAs. (ii) IEEE database, as the most important online academic research for power systems, unregarded these SBOAs in the solution process of the optimization problem. This is due to the lack of some desired capabilities, such as their limitation in the speed of convergence by comparison with other SBOAs, more complexities in the installation process, and excessive slowness for

achieving the best solution. As it seems, some SBOAs, such as ABC, PSO, GOA, GWO, and GOA, as well-considered algorithms, are utilized in electrical and power systems by attention to their NORP in IEEE database. Therefore, the authors, in the primary steps, selected them for tuning MPID controller through quasi – oppositional method in the output tracking control. They assure that this paper can consider as an elementary starting point in QO – SBO method and then it will be pursued by other new SBOAs in the future. In the following section, a general review will be presented about the performed SBOAs and after that, quasi-opposite – based learning method will be browsed as the main proposed

TABLE 1. (a) First part of online academic research about SBOAs from 1980 to 2017. (b) Second part of online academic research about SBOAs from 1980 to 2017.

SBOAs	Number of Relevant Papers		
	IEEE	Springer	Science Direct
Artificial Bee Colony Algorithm (ABC) [70]	67	119	456
African Buffalo Optimization (ABO) [77]	-	2	80
Ant Colony Optimization (ACO) [73]	44	486	678
Artificial Fish Swarm Algorithm (AFSA) [47]	4	35	23
Antlion Optimizer (ALO) [78]	6	10	14
Bat Algorithm (BA) [79]	28	189	756
Bees Algorithm (BA*) [80]	9	56	863
Beaver Algorithm (BA**) [81]	-	2	30
Bumble Bees Mating Optimization (BBMO) [82]	-	2	-
Bee Colony Optimization (BCO) [83]	60	71	498
Bacterial Colony Optimization (BCO*) [84]	5	6	44
Bee Collecting Pollen Algorithm (BCPA) [85]	-	2	22
Bacterial Foraging Optimization (BFO) [86]	51	141	274
BeeHive (BH) [87]	-	35	23
Bees Life Algorithm (BLA) [88]	-	1	11
Bird Mating Optimizer (BMO) [89]	-	7	85
Bee System (BS) [90]	-	3	10
Bees Swarm Optimization (BSO) [91]	-	3	8
The Cat Swarm Optimization (CaTS) [92]	-	1	2
Cuckoo Search (CS) [93]	50	246	280
Chicken Swarm Optimization (CSO) [94]	1	8	41
Dragonfly Algorithm (DA) [95]	-	41	41
Dolphin Partner Optimization (DPO) [96]	-	1	12
Firefly Algorithm (FA) [97]	63	259	330
Frog Calling Algorithm (FCA) [98]	-	1	15
Fruit Fly Optimization Algorithm (FFOA) [99]	6	37	119
Fast Marriage in Honey Bees Optimization (FMHBO) [100]	-	1	7
Fish-Swarm Algorithm (FSA) [101]	8	41	330
Fish School Search (FSS) [102]	-	3	6
Group Escaping Algorithm (GEA) [103]	-	1	4
Grasshopper Optimization Algorithm (GOA) [61]	5	38	45
Glow-worm Swarm Optimization (GSO) [104]	-	4	6
Grey Wolf Optimizer (GWO) [68]	17	81	346
Honey Bee Algorithm (HBA) [105]	-	4	154
Honey Bee Foraging (HBF) [106]	-	6	95
Honey Bees Mating Optimization (HBMO) [107]	-	18	73
Hunting Search Algorithm (HSA) [108]	-	2	174
Krill Herd Algorithm (KHA) [109]	2	34	42
Marriage in Honey Bees Optimization (MBO) [110]	-	4	7
Moth-Flame Optimization (MFO) [111]	14	54	75
Mosquito Host-Seeking Algorithm (MHSA) [112]	-	2	39

TABLE 1. (Continued.) (a) First part of online academic research about SBOAs from 1980 to 2017. (b) Second part of online academic research about SBOAs from 1980 to 2017.

SBOAs	Number of Relevant Papers		
	IEEE	Springer	Science Direct
Migrating Birds Optimization (MiBO) [113]	-	2	6
Particle Swarm Optimization (PSO) [76]	747	1723	1843
Roach Infestation Optimization (RIO) [114]	-	3	10
Shuffled Frog Leaping Algorithm (SFLA) [115]	5	40	43
Slime Mould Optimization Algorithm (SMOA) [66]	-	-	4
Shark-Search Algorithm (SSA) [116]	-	1	13
Superbug Algorithm (SuA) [117]	-	1	5
Termite Algorithm (TA) [118]	-	2	10
Virtual Bee Algorithm (VBA) [119]	-	3	11
Wolf Colony Algorithm (WCA) [120]	3	2	18
Whale Optimization Algorithm (WOA) [121]	27	94	112
Wolf Pack Search Algorithm (WPS) [122]	2	-	71
Wasp Swarm Optimization (WSO) [123]	-	5	22

strategy in this paper. Then, the simulation results section will emphasize assessing the proposed tuning MPID method based on the obtained outcomes.

A. GRASSHOPPER OPTIMIZATION ALGORITHM (GOA)

The grasshopper optimization algorithm, which is firstly proposed by Saremi *et al.* [61], is one of the new well-satisfied, and famous SBOAs. To be clear, pliability, imitative-free mechanism, and local optima avoidance are the most important reasons behind the approval of GOA, like other applied SBOAs in this paper. The GOA structure is modeled based on the behavior of grasshopper swarms in nature. As it is defined correctly in [51], two impressive processes in optimization problems are exploration and exploitation of the search space. the grasshoppers supply these two stages during the food search through these social interactions.

By considering the above descriptions, it is possible to define the mathematical model utilized for achieving the behavior simulation of the swarm grasshoppers as follows:

$$X_i = S_i + G_i + A_i \tag{17}$$

where X_i shows the position of the i^{th} grasshopper, S_i is as the social interconnection, G_i is the gravity force of the i^{th} grasshopper and A_i specifies the wind advection. All of these randomized behaviors is mathematically presented as follows:

$$S_i = \sum_{\substack{j=1 \\ j \neq i}}^N s(|x_j - x_i|) \frac{x_j - x_i}{d_{ij}} \tag{18}$$

where s is a function to define the strength of social forces, as is presented in (19), N is the number of grasshoppers in a

swarm and d_{ij} indicates the distance between the i^{th} and j^{th} grasshopper.

$$s = f e^{-l} - e^{-r} \tag{19}$$

where f and l are two constants that indicate respectively the intensity of absorption and the attractive length scale, and r is a real value. Therefore, finally (17) can rewrite as follows:

$$X_i^d = c \left(\sum_{\substack{j=1 \\ j \neq i}}^N c \frac{ub_d - lb_d}{2} s(|x_j^d - x_i^d|) \frac{x_j^d - x_i^d}{d_{ij}} \right) + \hat{T}_d \tag{20}$$

where ub_d and lb_d show the upper and lower band in D - dimension, respectively. The main value for the D - dimension in the best-calculated solution so far, is called \hat{T}_d . Also, the coefficient c decreases the comfort zone proportional to the number of iterations and is obtained as follows:

$$c = c_{max} - l \frac{c_{max} - c_{min}}{L} \tag{21}$$

where the maximum and minimum values for c are introduced by c_{max} and c_{min} respectively. Also the current and the biggest number iterations are shown using l and L respectively.

B. GREY WOLF OPTIMIZATION ALGORITHM (GWO)

The other studied SBOA is called GWO which is based on the social hierarchy and hunting behavior of grey wolves [68]. The benefits of GWO are:

- (i) it helps to escape from the initialization of input parameters.
- (ii) it helps to be straightway and free from computational elaboration.
- (iii) it provides the facility of the transformation of such a concept to the programming language.
- (iv) It provides the simplicity of understanding.

It is available to model GWO algorithm through the social interconnection of grey wolves in nature, as the effective part of a swarm-based algorithm. Several applied power system problems are solved by utilizing GWO algorithm (such as [35]–[69]). Naturally, a swarm of wolves is categorized into individual types of members based on the command level containing alpha, beta, delta, and omega. The most impressive presiding wolf is alpha and this capability will be decreased from alpha to omega. The hunting process in wolves generally accomplishes as a swarm. On the other hand, wolves collaborate in an intelligent way to hunt a victim. The hunting process is begun by tracking the victim by Grey wolves as a team. Then they try to siege it circularly. This process will be pursued for achieving more chances in hunting.

For achieving a mathematical model from GWO, as it can emulate the hunting behavior of grey wolves, it is necessary to procreate a randomized swarm of wolves in the search space. Then utilize a , b , and d wolves to approximate the position of the victims. As for other wolves, they are commanded to determine the distance between themselves and the a , b , and d wolves, and after that, they get close to the victim and encompass it. In the end, they catch the victim successfully. These comprehensive stages are indicated in Figure 6.

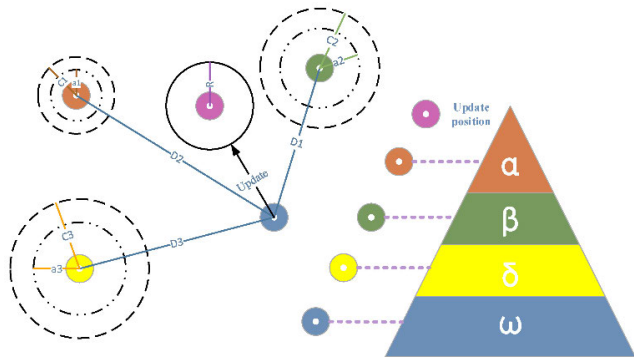


FIGURE 6. The conceptual block diagram for GWO algorithm.

It is possible to generate a mathematical model as follows:

$$\vec{D} = |\vec{C} \cdot \vec{X}_p(\text{iter}) - \vec{X}(\text{iter})| \quad (22)$$

$$\vec{X}(\text{iter} + 1) = \vec{X}_p(\text{iter}) - \vec{A} \cdot \vec{D} \quad (23)$$

where $\vec{X}(\text{iter} + 1)$ emphasizes the new position of the wolf. Therefore, $\vec{X}_p(\text{iter})$, by subscript p , illustrates the current location of the victim. Based on (22) and (23), to determine \vec{A} and \vec{C} , as defined coefficients, the equations can be rewritten as follows:

$$\vec{A} = 2\vec{a} \cdot \vec{r}_1 - \vec{a} \quad (24)$$

$$\vec{C} = 2\vec{r}_2 \quad (25)$$

The distance, which indicates the location of the victim, will be named by \vec{D} . Also \vec{a} is a setting parameter that decreases linearly from 2 to 0 among the procedure. Also two randomized parameters, \vec{r}_1 and \vec{r}_2 , are generated from the

interval 0 to 1. In the hunting procedure which is led by α , the positions of the wolves are upgraded. Despite α is the most impactful agents in the hunting phase, as yet sporadically β and δ also cooperate in this process. To find the best positions, the three optimized solutions (determined so far) in terms of α , β , and δ are fixed and the remaining solutions including ω challenge. Following equations are utilized to upgrade:

$$\vec{D}_\alpha = |\vec{C}_1 \cdot \vec{X}_\alpha - \vec{X}|, \quad \vec{D}_\beta = |\vec{C}_2 \cdot \vec{X}_\beta - \vec{X}|, \quad \vec{D}_\delta = |\vec{C}_3 \cdot \vec{X}_\delta - \vec{X}| \quad (26)$$

$$\vec{X}_1 = \vec{X}_\alpha - \vec{A}_1 \cdot \vec{D}_\alpha, \quad \vec{X}_2 = \vec{X}_\beta - \vec{A}_2 \cdot \vec{D}_\beta, \quad \vec{X}_3 = \vec{X}_\delta - \vec{A}_3 \cdot \vec{D}_\delta \quad (27)$$

$$\vec{X}(\text{iter} + 1) = \frac{\vec{X}_1 + \vec{X}_2 + \vec{X}_3}{3} \quad (28)$$

It would be indicated that the final position is random naturally among the circle which is completely described by α , β , and δ in the search space, while the other wolves upgrade their position by approximating the victim position.

C. ARTIFICIAL BEE COLONY ALGORITHM (ABC)

One of the high-trusted and well-satisfied swarm-based meta-heuristic algorithms is Artificial Bee Colony (ABC) [70]. In this SBOA, like some other algorithms, the most determinative factor for constructing the effective exploitation and exploration process is the operation of the honey bees foraging. The obtained different experiences demonstrate to be well-satisfied with the ABC algorithm for the solution of the multidimensional optimization problems (such as [71]). The bee population is classified into three main groups which work in the colony: (i) employed, (ii) onlooker, and (iii) scout bees. There are three important stages in the search procedure. At first, randomly the food sources are chosen as the initial target movement for the employed bees. Therefore, these surrounded sources are considered as a possible solution for the optimization process. After that, it will be available to determine the value of the objective function by utilizing the nectar amount of the food source. The obtained value for this objective function represents the quality of the solution. The onlooker bees are situated to the food source through probability-based choice. In fact in this method, the better value for the objective function will be equal to the higher the probability of onlooker bees choosing that specific food source. The most important scheme for upgrading the food source position is the greedy selection. The modification process for the position selection of the food source is achieved using the employed bees. So the comparison process of the objective function value of the modified solution is utilized with the previous objective function value. If the improved solution of the objective function value is higher, the improved food position and objective function value will be upgraded, substituting the previous values. It is possible to generate the modified food solution utilizing the following equation:

$$P_{ij} = X_{ij} + \theta_{ij} (X_{ij} - X_{ik}) \quad (i \neq k) \quad (29)$$

where the current iteration is named by i and random digits as j and k , are selected while $j, k \in [-1, 1]$. According to (29), it is obvious when the distance between X_{ij} and X_{ik} is decreased, the changes attached with the food source, X_{ij} will be reduced. This decreased process will be eventuated the ABC narrow down to the solution step by step using decreasing the step size as the optimized solution approaches. Therefore, the improved parameter, P_{ij} will be utilized as the modified food source for more evaluation. Also, a food source is chosen according to the possibility of the food source, ξ_i , using the onlooker bee, as follows:

$$\xi_i = \frac{\alpha F_i}{(\max\{F_g\}) + \beta}, \quad F_g = \{F_i, F_{i+1}, F_{i+2}, \dots, F_k\} \quad (30)$$

where the fitness value of solution i as assessed by the employed bees is named F_i and the maximum fitness value for the general fitness derived from the employed bee section, F_g , is named $\max\{F_g\}$. Also, k in (30) indicates the total number of food sources. The randomized numbers, α and β , in (30) indicate the variables which are considered in $[0, 1]$ while α is 0.9 and β is 0.1 ($\alpha + \beta = 1$) [72]. The exploitation of the food sources is performed using the employed and onlooker bees. After that, the exploration of the food sources is lead to raise the onlooker bees through the scout bee phase. It is possible to abandon the food source when the position of the food source cannot be modified using a specified number of cycles. Then a fresh food source, which is randomly produced using the scout bee phase, will be replaced with the abandoned food source. So this substituted food source is evaluated using the scout bee phase to characterize if a better solution exists figured out to the current solution. Finally, the food position and objective function are upgraded if a better solution exists.

The ability scheme of the local and global search will be augmented by the greedy selection scheme and the random selection scheme. According to the above descriptions, a conceptual flowchart indicated the ABC algorithm in Figure 7.

D. ARTIFICIAL FISH SWARM ALGORITHM (AFSA)

Naturally, singular search or tracking the other fish can aid a fish to find the more nutritious area. Simulation of the fish treatment, including hunting, crowding, and tracking with the local search of individual fish for achieving the global optimum, is considered as the main concept of the AFSA [47]. The living environment of a fish is regarded as the solution space and the states of other fish.

The next treatment of fish pertains to its current state and its local environmental state. The environment of a fish will be impressed through its individual and companion’s activities. This algorithm has resembling attractive characteristics of genetic algorithm (GA), such as non-aligned from gradient data of the objective function, the capability to dissolve intricate non-linear high dimensional problems. Also, they converge faster than other similar cases and need few parameters

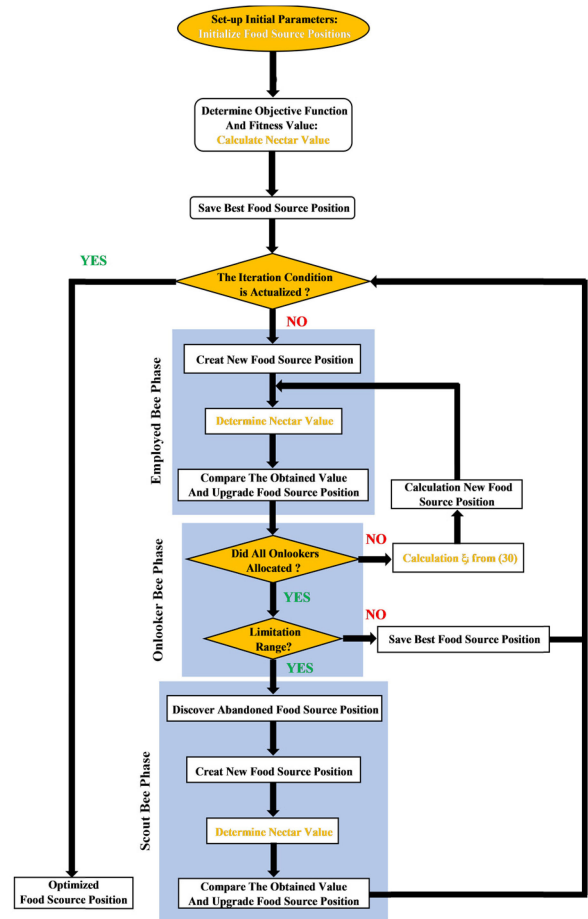


FIGURE 7. The conceptual block diagram for ABC algorithm.

to be tuned. While AFSA hasn’t the crossover and mutation procedure applied in GA, so it could be worked more easily.

Artificial fish (AF) is a fictitious entity of true fish, which is utilized to continue the analysis and clarification of the problem and can be perceived through the animal ecology concept. It is possible to consider an AF as an entity summarized with a collection of treatments and individual information through the object-oriented analytical method.

Assume $X = (x_1, x_2, \dots, x_d)$ is the current position of an AF. The maximum step-length that a fish can take in every motion, is named using (S or Step). Also, the visual distance is introduced by V and therefore X_v designates the visual position. In addition, the location of the companions inside the visual distance of the current AF is considered as X_{n1} , X_{n2} , and X_{n3} . Each AF investigates the search space around its vision distance. If a new position is better than its current location, it goes a step toward that position. Consider that $Y = f(X)$ indicates the food attentiveness of the AF at the current position, where the objective function is called by Y. By considering the above descriptions, Figure 8 indicates a view of an AF and its environment.

The general treatment of an AF can be described in four different classifications as follows:

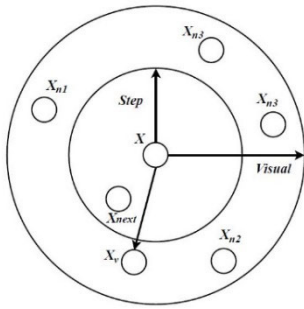


FIGURE 8. An AF with its environment.

1) HUNTING PROCESS

It can dare say that hunting treatment is the main applied process for a fish for achieving a location with the highest attentiveness of food. This treatment can be simulated through a radius of the neighborhood of a fish. Assume $X_i^{(t)}$ is considered as the current position of the i^{th} AF and also X_j be a state of an AF which is chosen randomly through the visual distance of the i^{th} AF as follows:

$$X_j = X_i^{(t)} + V \cdot rand \tag{31}$$

where the visual distance of the AF is called V and $rand$ indicates a random vector with each element between 0 and 1. In following the hunting process:

if ($Y_i < Y_j$)

$$X_i^{(t+1)} = X_i^{(t)} + S \cdot rand \cdot \frac{X_j - X_i^{(t)}}{\|X_j - X_i^{(t)}\|} \tag{32}$$

else

$$X_i^{(t+1)} = X_i^{(t)} + V \cdot rand$$

end

2) SWARMING PROCESS

Naturally, the tendency of the assembling is a conventional feature in each swarm. This swarm-based characteristic helps the animals to preserve themselves from danger while preventing over-crowded areas. Assume the sum of AFs indicates using n , also the number of companions inside the visual distance of the i^{th} AF is shown by n_f . Then the central position for the D-dimension space is called $X_c = (x_{c1}, x_{c2}, \dots, x_{cd})$ where x_{cd} is defined as follows:

$$x_{cd} = \frac{1}{n_f} \left(\sum_{j=1}^{n_f} x_{jd} \right) \tag{33}$$

If the described constraints in (34) are persuaded,

$$\begin{cases} Y_c > Y_i \\ \frac{n_f}{n} > \delta \end{cases} \tag{34}$$

where the swarming coefficient is called δ , this denotes that there is more food in the center, and the area is not over-swarmed. In such situations:

It is important that the hunting process will be accomplished if: (i) the denoted constraints in (34) are not satisfied (ii) there is no companion inside the visual distance of the i^{th} AF (or $n_f = 0$).

3) TRACKING PROCESS

The tracking stage takes place when a fish discover a location with a better concentration of food, other fishes track. So in this process:

$$\text{if } (Y_i < Y_j) \ \&\& \ \left(\frac{n_f}{n} < \delta \right) \left\{ \begin{array}{l} \% X_j \text{ contains more food} \\ \text{and} \\ \% \text{ it is not over-swarmed} \end{array} \right. \tag{35}$$

$$X_i^{(t+1)} = X_i^{(t)} + S \cdot rand \cdot \frac{X_j - X_i^{(t)}}{\|X_j - X_i^{(t)}\|}$$

else

The hunting Process is executed

end

4) RANDOM TREATMENT

As it was indicated about the ABC algorithm, foraging is the common, main and random activity within all swarm-based animals which is led to create an intelligent approach. The random treatment authorizes an AF to search for food or to track a swarm in a larger space. On the other hand, the random treatment for an AF happens when none of the relevant indexes to the hunting, swarming, and tracking treatments are persuaded. Therefore, the AF chooses a random state inside its visual distance, as follows:

$$X_i^{(t+1)} = X_i^{(t)} + V \cdot rand \tag{36}$$

Generally for the AFSA, the equivalent factor between exploration and exploitation is managed through δ , V , and S . The exploration capability will be increased using a selection of larger δ , V , and S values.

E. PARTICLE SWARM OPTIMIZATION (PSO) ALGORITHM

This strategy, in the improvement trajectory of the earliest SBOAs, Ant Colony Optimization (ACO) [73], [74], was constituted and gradually was accepted as the most high-applied and well-trusted in all scientific societies [75]. The swarm of applicant solutions within the optimization process is selected as the main particles in the PSO algorithm. In this methodology, the vector of position and velocity, are enumerated as the main components for each one of the particles. Also, the Newtonian approach is achieved to guide every particle inside towards the global optimum. To prevent the repetition of similar concepts and equations in this section, the authors prefer studying the above references and also [76], for achieving the performance and applications of PSO in the optimization process.

V. QUASI OPPOSITIONAL – BASED LEARNING

Indubitably, one of the most tangled knots in SBOAs is to neglect to jump out from local minima. Therefore by considering this problem, it is impossible to achieve the best feasible optimized solution. Step by step, several expansive auxiliary methods have been introduced to overcome this complication [124]–[126]. For the first time, Tizhoosh, enhanced the evolutionary trajectory by introducing of oppositional-based learning (O-BL) strategy [127]. Therefore, O-BL was expanded to enhance the applicant solution by considering the current population besides its opposite population at the same time. If $x(x_1, x_2, \dots, x_D)$, is assumed as $x_i \in [\alpha_i^{lb}, \beta_i^{ub}]$ and x_i are real numbers in a D-dimensional space, then its opposite number, x^o , is defined as follows:

$$x_i^o = \alpha_i^{lb} + \beta_i^{ub} - x_i \quad (i = 1, 2, 3, \dots, D) \quad (37)$$

The above definition of the opposite point is described based on the relationship between points in the search space without considering their target values. Figure. 9 shows x and its opposite, x^o , in different dimensional spaces.

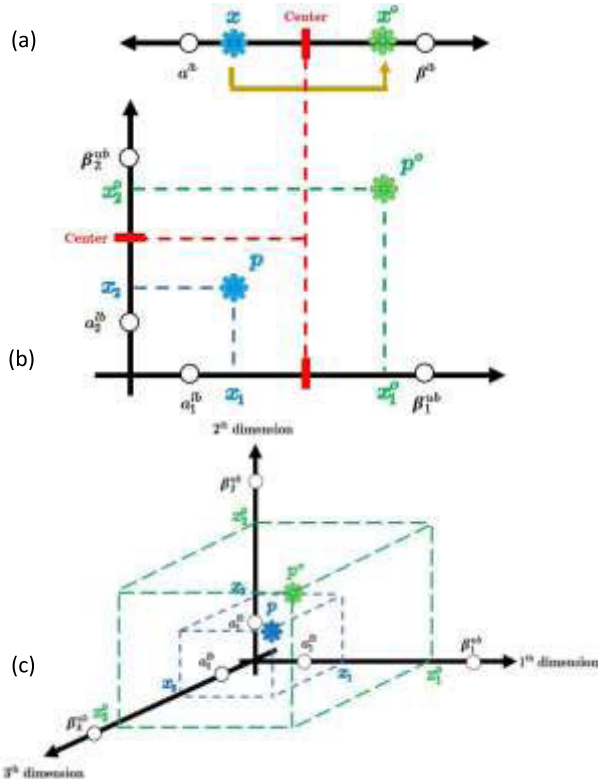


FIGURE 9. The placement point x and its opposite, (a) In 1st dimension space, (b) in 2nd dimension space, (c) in 3rd dimension space.

SBOAs are begun by the initial population and focus on enhance them toward some optimal solution. The process of searching concludes when some predefined criteria are assured. The process is begun with random guesses in the absence of a priori data about the solution.

This work can be amplified by beginning with a closer i.e. fitter solution by exactly the opposite solution. By considering O - BL method, the fitter one (guess or

opposite guess) may be selected as an initial solution. The basis of the theory of probability, half of the time value, a guess is farther from the solution than its opposite guess. So the process begins with the closer of the two guesses. The duplicate method can be approached not only to the initial solution but also continues to each solution in the current population.

For the first time, Rahnamayan *et al.* [128] presented Quasi-Oppositional (QO) based learning method for more achieving to the applicant solution by attention to the current population additionally its quasi-oppositional at the same time. As it seems SBOAs by this method can provide a quasi-opposite number which is usually closer than a random number to the solution. Also, it was proved that a quasi-opposite number is usually closer than an opposite number to the solution [129]. In this paper, the authors have tried to utilize the QO technique for both preprocessing, including population initialization and generation jumping.

As it was defined in O-BL about the opposite of a real number in D-dimensional space, for any real number, like $x(x_1, x_2, \dots, x_D)$, subject to $x_i \in [\alpha_i^{lb}, \beta_i^{ub}]$, its quasi-opposite number, x^{qo} , is introduced as follows:

$$x_i^{qo} = \text{rand} \left(\frac{\alpha_i^{lb} + \beta_i^{ub}}{2}, x_i \right) \quad (i = 1, 2, 3, \dots, D) \quad (38)$$

As it was mentioned, it is possible to attain more suitable applicant solutions QO-based population initialization may achieve fitter candidate solutions as the concurrent consideration of the randomly caused initial positions and their quasi-opposite positions enhance the quality of the initial population and speeds up the search process by exploring the robust regions of the search space. The constructional-code of QO-based population initialization is attended as follows:

A. CONSTRUCTIONAL-CODE FOR QO-BASED POPULATION INITIALIZATION

Generate initial random population: x

```

For  $i = 1: N_{pop}$  % the population size is called  $N_{pop}$ 
    For  $j = 1: D_p$  % the dimension of problem is  $D_p$ 
         $x^0(i, j) = \alpha^{lb}(1, j) + \beta^{ub}(1, j) - x(i, j)$  % the opposite of  $x$  is called  $x^0$ 
         $C(i, j) = \alpha^{lb}(1, j) + \beta^{ub}(1, j)/2$ 
        if  $(x(i, j) < C(i, j))$ 
             $x^{qo}(i, j) = C(i, j) + (x^0(i, j) - C(i, j)) \times \text{rand}$  % the quasi opposite of  $x$  id  $x^{qo}$ 
        else
             $x^{qo}(i, j) = x^0(i, j) + (C(i, j) - x^0(i, j)) \times \text{rand}$ 
        end
    end
end
    
```

The optimization procedure may be enforced to skip based on jumping rate, J_r , to a new applicant solution that is more compatible than the current one. After producing a fresh population-based on J_r , the quasi-opposite population is estimated and the most suitable population gets classified from

the union of current and quasi-opposite population-based on applicant solution. In this research, the time-varying jumping rate is calculated as follows:

$$J_r = \frac{\Delta J_r \times \text{NFR}}{\text{NFR}_{\max}} \quad (39)$$

where $\Delta J_r = J_r^{\max} - J_r^{\min}$ and NFR is the number of function recall at the current iteration. In the following paper, the jumping rate is considered as $J_r \in [0, 0.4]$. Therefore, the constructional-code of QO-based generation jumping is exhibited as it shows:

B. CONSTRUCTIONAL-CODE FOR QO-BASED GENERATION JUMPING

Calculate jumping rate from (40): J_r

```

If (rand <  $J_r$ )
  For  $i = 1: N_{pop}$  % the population size is called  $N_{pop}$ 
    For  $j = 1: D_p$  % the dimension of problem is  $D_p$ 
       $x^0(i, j) = \alpha^{lb}(1, j) + \beta^{ub}(1, j) - x(i, j)$ 
      % the opposite of  $x$  is called  $x^0$ 
       $C(i, j) = \alpha^{lb}(1, j) + \beta^{ub}(1, j) / 2$ 
      if ( $x(i, j) < C(i, j)$ )
         $x^{qo}(i, j) = C(i, j) + (x^0(i, j) - C(i, j)) \times \text{rand}$ 
        % the quasi opposite of  $x$  id  $x^{qo}$ 
      else
         $x^{qo}(i, j) = x^0(i, j) + (C(i, j) - x^0(i, j)) \times \text{rand}$ 
      end
    end
  end
end
end

```

It is considered that in the present work, as it was explained, the quasi-oppositional method is selected for all utilized SBOAs, including QO-GWO, QO-GOA, QO-ABC, QO-AFSA, and QO-PSO, as the main way for preparing (population initialization and generation jumping) swarm-based methods. Figure. 10 illustrates x and its quasi-opposite, x^{qo} , in all three-dimensional spaces.

VI. CONVENTIONAL MPID CONTROLLER DESIGN

The typical tuning process of an MPID controller, conventional MPID which is called C-MPID in all simulation results, for a linear multivariable stable plant is introduced in [130]. Fig.8 indicates a structure from applied C-MPID in this paper. Therefore, the obtained C-MPID controller coefficients from this method are calculated based on the bandwidth frequency, ω_B . Accordingly, the interaction is decreased and a suitable decoupling characteristic is obtained around the frequency. After all, it is important to note that this typical method is not an easy task to be utilized practically for frequency analysis. In this method, for achieving the C-MPID controller, $G_C^{\text{Typical}}(s) = k_p^{\text{typical}} + \frac{k_i^{\text{typical}}}{s} + k_d^{\text{typical}}s$, the proportional, integral feedback, and derivative gains are calculated from:

$$\begin{aligned} k_p^{\text{typical}} &= \rho G_{\text{Tf}}^{\text{ESS}}(j\omega_B)^{-1}, \\ k_i^{\text{typical}} &= \mu G_{\text{Tf}}^{\text{ESS}}(j\omega_B)^{-1}, \\ k_d^{\text{typical}} &= \delta G_{\text{Tf}}^{\text{ESS}}(j\omega_B)^{-1} \end{aligned} \quad (40)$$

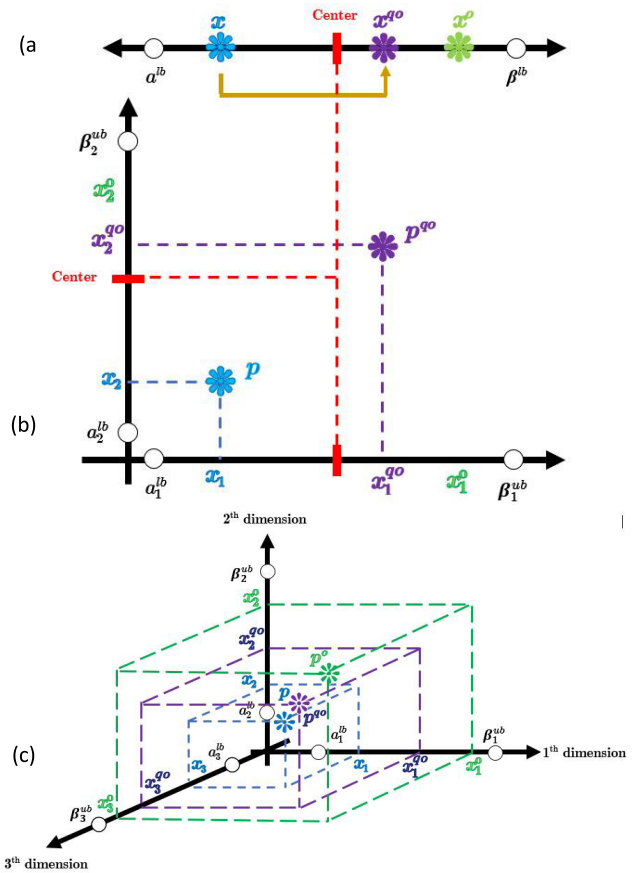


FIGURE 10. The placement point x and its quasi - opposite, (a) In 1st dimension space, (b) in 2nd dimension space, (c) in 3rd dimension space.

where ρ , μ and δ are the tuning parameters. By considering a complex gain obtained from the calculation of $G_{\text{Tf}}^{\text{ESS}}(j\omega_B)^{-1}$, a real approximation of $G_{\text{Tf}}^{\text{ESS}}(j\omega_B)^{-1}$ is necessary which can be done by solving the following optimization problem as follows:

$$M(N, \emptyset) = \left[G_{\text{Tf}}^{\text{ESS}}(j\omega_B)N - e^{j\emptyset} \right]^T \left[G_{\text{Tf}}^{\text{ESS}}(j\omega_B)N - e^{j\emptyset} \right], \quad (41)$$

where N and \emptyset are two constant parameters that are utilized to minimize M [130].

As it was described, FIGURE 11. indicates the general structure which is performed for tuning C-MPID controller and comparing it with the proposed QO-SMPID in this paper.

VII. PROPOSED OBJECTIVE FUNCTION

To evaluate the performance of SBOAs in finding the best coefficients of MPID for AC/HVDC with the ESS, at first, it is necessary to propose a new cost function according to desired MIMO characteristics. The utilized minimization process, which is introduced in this section, is achieved using SBOAs for the proposed cost function and it will be compared with C-MPID method as explained in Section VI.

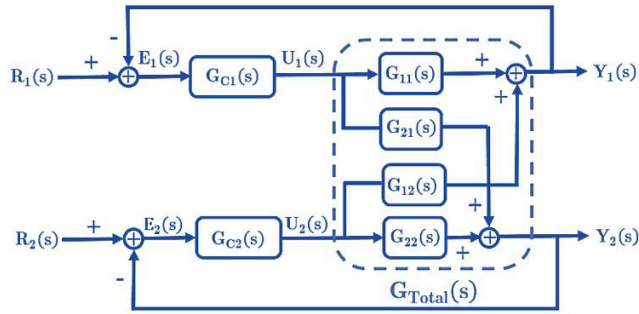


FIGURE 11. Typical MIMO block diagram for 2 inputs and 2 outputs.

A. INTRODUCTION OBJECTIVE FUNCTION TERMS

This part is concentrated on finding a suitable and strong method for the optimization process. By considering the derived features of step response and its availability in every iteration of the simulation, an objective function is utilized according to the required features of the step function. So the calculation procedure of the fitness index is centralized on the determined MIMO transfer function in this part.

On the other hand, the applied objective index is a function that contains the summation of selected step response features as a linear combination by weighted coefficients. The proposed features, which are mentioned in this work, are described as follow:

1) STABILITY INDEX (SI)

One of the most impressive factors in all linear systems, that can challenge stability, is the movement manner of closed-loop poles. As it is cleared, the nature of a linear steady-state model can be affected by the pole placement process in the s. Therefore, in this work, the authors are going to present a new approach based on the step response manner for achieving another stability index based on the poles' behavior during the optimization process. The described above details persuade the authors to redefine and utilize a new systemical index based on the step response behavior which is obtained from the calculated transfer function of the investigated system.

For achieving this component, firstly it is necessary to consider the real value of poles. Then, it can be noted that the most positive value between the obtained reals with determining their maximum is selected. As we know, when these poles locate on the imaginary axes or in the right hand of s (unstable poles), the calculated parameter will be zero or bigger than zero. To conquer this problem, we can write:

$$Max_i^p = \max \{ \text{Real}(p_1), \text{Real}(p_2), \dots, \text{Real}(p_i) \} \quad (42)$$

where p_1, p_2, \dots, p_i are the obtained closed-loop poles in (42). So:

$$MaxReal_i^p = \min \{ Max_i^p, 0 \} \quad (43)$$

On the other hand, if there is an unstable pole or a closed-loop pole locates on the imaginary axes, by attention to (43), the MaxReal value will be equal to zero. Also by considering (43), the maximum real part of closed-loop poles will

be negative or in the worst possible case equal to 0. Now, the stability index (SI) parameter can be described as follows:

$$SI = \frac{-1}{MaxReal_i^p} \quad (44)$$

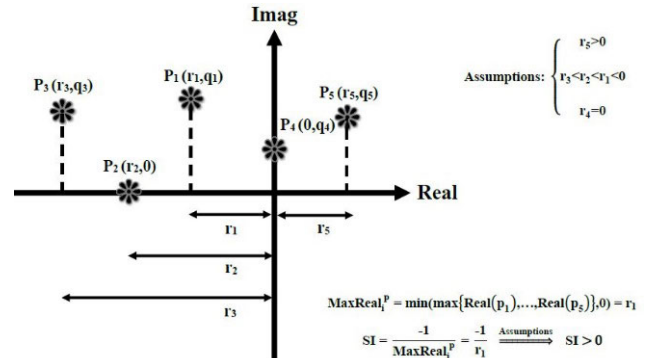


FIGURE 12. The calculation form of SI parameter by (45).

Figure 12, indicates the pole placement of a system with 5 different closed-loop. This figure shows that one of these poles locates on the half-right side of s. Also, one pole locates on the imaginary axes. Based on the described explanations, SI parameter will be calculated in this figure.

2) SETTLE TIME INDEX (ST)

Indisputably, the minimum time that the amplitude gets to correct the error of 0.05, as the settling time index, is one of the highest risk factors for step response in a system. On the other hand, based on (12), AC/HVDC with ESS model, as the main plant, has a MIMO transfer function. Then by utilization of the step unit function, as the input signal, the obtained step response will be determined in a 2×2 matrix form.

Therefore, in this paper, the authors encounter four ST parameters which everyone belongs to one of the element matrices of the step response. Therefore, it seems that for MIMO step response:

$$ST^{MIMO} = \begin{bmatrix} ST_{11} & ST_{12} \\ ST_{21} & ST_{22} \end{bmatrix} \quad (45)$$

Actually, by attention to the worst possible situations, and the obtained elements of the matrix in (45), this index can be calculated:

$$ST = \max \{ ST_{ij} \} \quad (46)$$

3) RISE TIME INDEX (RT)

The final impressive factor of step response, which is used as the third term in the proposed objective function, will be introduced as the time it takes for the response to rise from 10% to 90% of the steady-state response. Correspondingly, there is a matrix for the calculated RT as follows:

$$RT^{MIMO} = \begin{bmatrix} RT_{11} & RT_{12} \\ RT_{21} & RT_{22} \end{bmatrix} \quad (47)$$

And finally, the third index will be determined as it follows:

$$RT = \max\{RT_{ij}\} \quad (48)$$

Therefore, based on (44), (46), and (48), the objective function can be introduced as a linear combination of the above indexes:

$$Z = k_1 \times (SI) + k_2 \times (ST) + k_3 \times (RT) \quad (49)$$

where $k_1, k_2,$ and k_3 are constant and real positive digits which are chosen based on the aim design. By considering these constant digits, it will be changed the duty of every above index in the minimization process of the objective function. It is notified that in this case, the authors sorted out all k_i are equal to 1. As it seems in (49), the objective function is generated by three terms with the same dimension. Therefore, SBOAs, including GOA, GWO, ABC, AFSA, and PSO will be accomplished by execution of this objective function during the optimization procedure. FIGURE 13. indicates a conceptual block diagram from the optimization process by the proposed objective function.

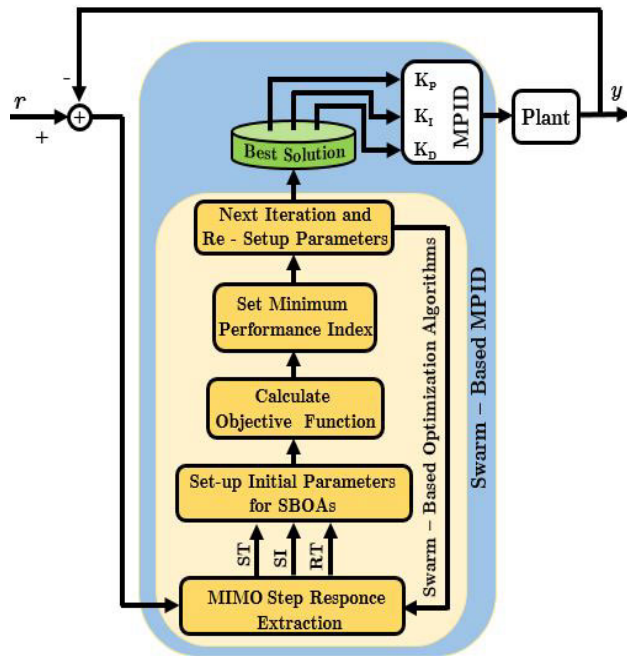


FIGURE 13. The proposed SMPID controller block diagram.

VIII. IMPLEMENTATION OF QO STRATEGY ON SBOAs

As it was described in the previous sections, the main idea of the authors is to apply QO strategy on SBOAs for tuning MPID controller in the output tracking control process. Therefore, an algorithmic trajectory is presented to implement this method and install QO-SMPID according to the following applied steps:

Step 1) Initialize the input parameters of the selected SBOAs, such as population size and the number of iterations.

Step 2) Set the preparation parameters of QO strategy, such as the minimum and the maximum jumping rate (J_r^{max} and J_r^{min}).

Step 3) Prepare swarm, such as the search agents generation randomly.

Step 4) Calculate the proposed objective function, based on (50).

Step 5) Determine quasi-opposite population at the calculated search space and opposite population using (38).

Step 6) Return to Step 4 and calculate the objective function by attention to described changes in Step 5.

Step 7) Upgrade and refresh the positions according to the main mathematical equation for the selected SBOAs.

Step 8) Assess the feasibility of the recently produced solution.

Step 9) Exchange infeasible solution by the randomly produced new solution.

Step 10) Generate a quasi-opposite population based on the defined jumping rate.

Step 11) Assort the positions of the calculated search agents among Step 10 from the best to worst value and utilize the determined values in Step 11 for the next generation.

Step 12) Return to Step 7 while the termination index is met.

IX. SIMULATION RESULTS AND DISCUSSION

According to the explanations in the previous section, the main goals of this section are as follows:

- To evaluate the flexibility, velocity, and accuracy in the performance of the proposed output tracking control by considering a high-challenged scenario for the reference inputs. It is also useful to consider the variation of the tested MIMO outputs, two outputs related to MIMO features, with tie-line AC power between the areas ($\Delta P_{tieAC12}$).
- To digitize the obtained simulation results for more suitable comparison among the applied SBOAs and also following the variation of all terms of the objective function.
- To investigate the structural stability assessment by considering small deviations in the main constants of AC/HVDC model with ESS, such as the control parameters and the robustness performance.
- To compare the characteristics performance of the proposed objective function with the standard index, such as integral time absolute error (ITAE).

A. PERFORMANCE ASSESSMENT OF PROPOSED SMPID

One of the best ways for achieving the accurate evaluation of the proposed output tracking control is the flexibility assessment of the obtained output. Therefore, the authors defined the main scenario by attention to deviation in the reference input signal shown in Figure 14. In the following part, the proposed scenario will be realized by the tuned SMPID through QO strategy.

The selected SBOAs for implementation in this work are GWO, GOA, AFSA, ABC, and PSO. Then, the obtained simulation results will be compared with the conventional MPID (C-MPID) controller. This part is concentrated on finding

TABLE 2. The performance analysis of the main scenario on SBOAs.

SBOAs QO-SBOAs	Tuned MPID Coefficients *						Objective Value	Z		
	K _{p11}	K _{p22}	K _{i11}	K _{i22}	K _{d11}	K _{d22}		SI	ST	RT
GWO	1.1919	-0.0915	0.1452	-0.7391	-0.7276	0.125	751.3	62.608	500.8667	187.825
QO - GWO	1.1687	-0.0915	0.1763	-0.0415	-0.3142	0.1511	720.1	60.008	480.0667	180.025
GOA	1.1535	-0.0915	0.1762	-0.0799	-0.2709	-0.2866	760.9	63.408	507.2667	190.225
QO - GOA	1.2268	-0.0915	0.1437	-0.4437	-0.1485	-0.3286	745.1	62.091	496.7333	186.275
AFSA	1.1528	-0.0915	0.1740	0.0942	0.5660	0.7604	759.6	63.3	506.4	189.9
QO - AFSA	1.1604	-0.0915	0.1827	0.0989	0.5943	0.7984	720.4	60.033	480.2667	180.1
PSO	1.1539	-0.0915	0.1742	0.0668	0.0832	0.1058	755.5	62.958	503.6667	188.875
QO - PSO	1.2171	-0.0915	0.1403	-0.1183	-0.1194	0.2997	750.1	62.508	500.0667	187.525
ABC	1.1609	-0.0915	0.1575	-0.0810	0.2854	0.3813	740.5	61.708	493.6667	185.125
QO - ABC	1.1628	-0.0915	0.1703	0.0911	0.2285	0.2146	731.6	60.966	487.7333	182.9

$$* K_P^{ESS} = \begin{bmatrix} K_{p11} & 0 \\ 0 & K_{p22} \end{bmatrix}, K_I^{ESS} = \begin{bmatrix} K_{i11} & 0 \\ 0 & K_{i22} \end{bmatrix}, K_D^{ESS} = \begin{bmatrix} K_{d11} & 0 \\ 0 & K_{d22} \end{bmatrix} \xrightarrow{\text{Subject to}} -1.5 \leq K_{p,i,d(ii)} \leq 1.5$$

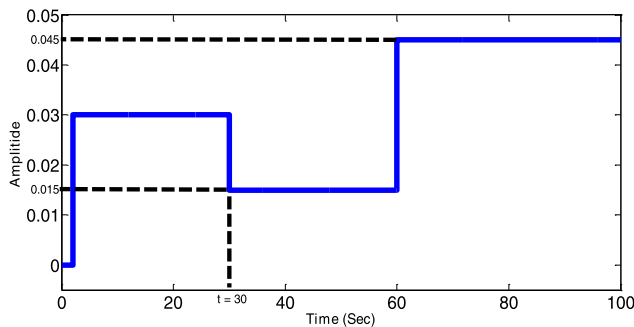


FIGURE 14. The reference input signal for the main scenario.

a suitable and strong method for the optimization process. By considering the derived features of step response and its availability in every iteration of the simulation, an objective function is utilized according to the required features of the step function.

B. SIMULATION SCENARIO

For achieving a more accurate assessment about the proposed tuning SMPID controller among the output tracking control process, cascaded changes have happened as shown in Figure 14. In this way, both under and over-frequency events can be considered for assessing the performance of the controller on tracking the step responses.

Firstly, original SBOAs are prepared to tune MPID controller parameters, and also QO strategy is utilized in SBOAs to precipitate their convergence velocity and computational performance. Because of the randomized nature of the optimization process, the various individual trial is necessitated to employ to extract the best solution. The comprehensive analysis with various population sizes in all selected SBOAs indicates that for a higher amount of population sizes such as 50, 60, 70, and 80, the objective value and its terms (SI, ST, and RT) are closed

equal to those amounts which are calculated at population size = 50.

Therefore, according to the obtained results, the authors considered that the selected SBOAs can present more acceptable outcomes by definition of the population size equal to 50 among the optimization process. Table 2, emphasizes the final tuned MPID coefficients for all considered SBOAs.

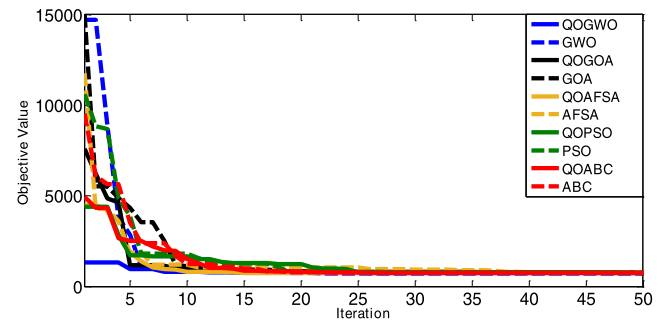


FIGURE 15. The convergence trajectory of the objective function.

Figure 15, shows the variation of the objective function among the tuning process of MPID using the proposed SBOAs by considering QO strategy. As shows that the population size equal to 50, will lead to suitable and unreplicative objective values.

Table 2, indicates the final setting MPID parameters for all considered SBOAs in the considered population size.

By attention to the variation of the objective function, Figure 15, it can be observed that the convergence speed in QO-SBOAs is better than the conventional SBOAs. Also, by attention to Figure 15, it seems that GWO has active participation in the convergence trajectory in comparison with other SBOAs.

Figures 16 and 17, indicate the results of the implementation of the tracking control trajectory through the

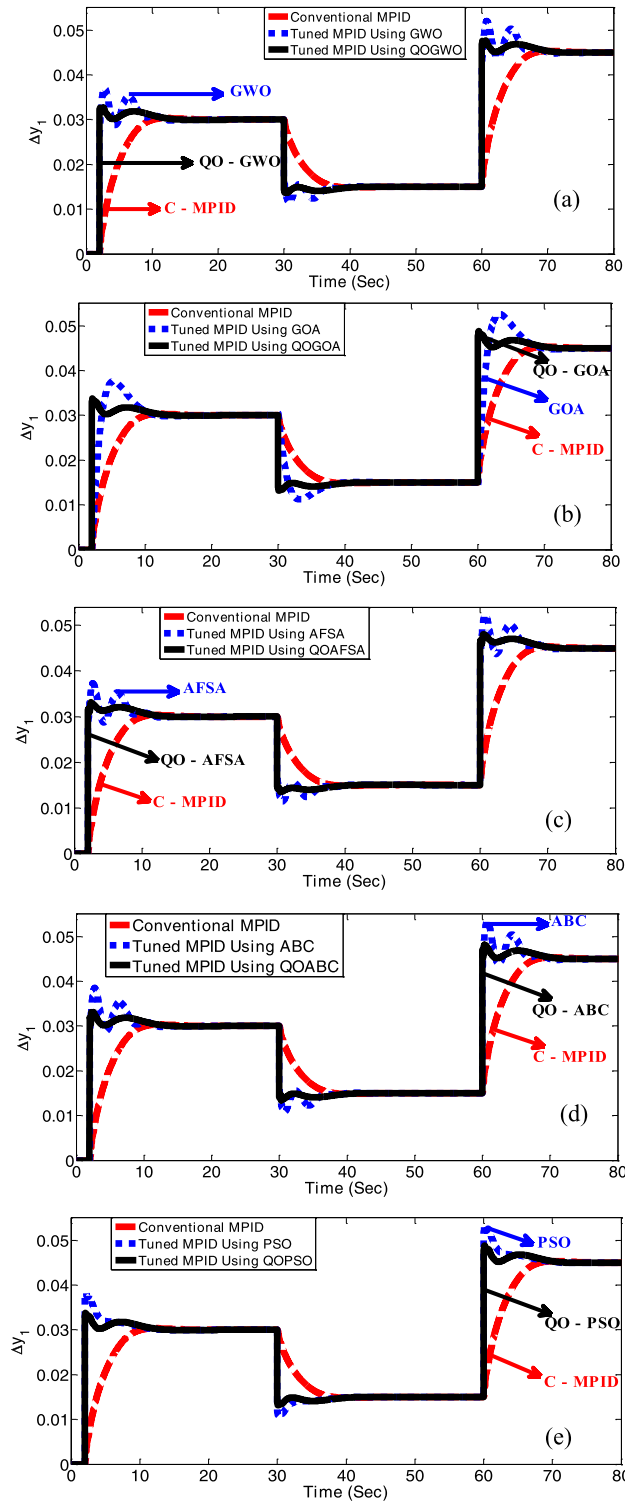


FIGURE 16. Tracking Trajectory on the First Output Using Proposed Method: (a) By GWO and QO – GWO, (b) By GOA and QO – GOA, (c) By AFSA and QO – AFSA, (d) By ABC and QO – ABC, (e) By PSO and QO – PSO.

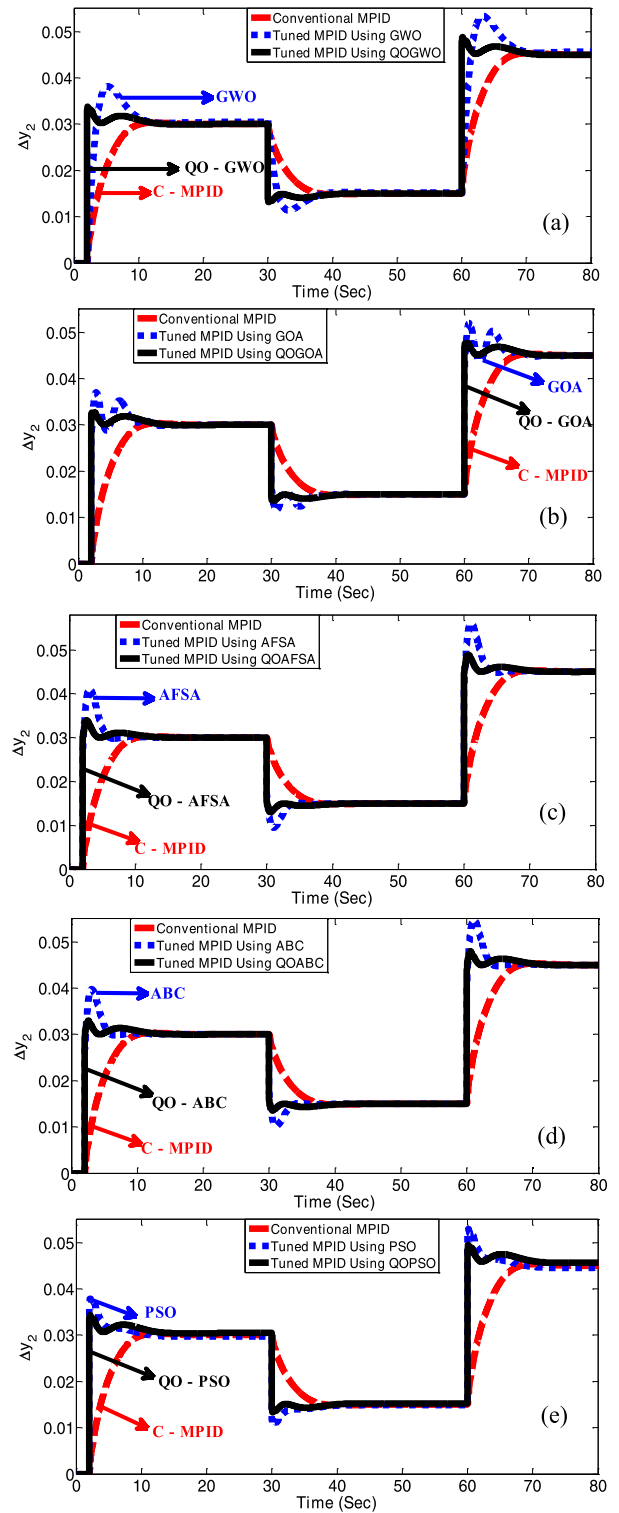


FIGURE 17. Tracking Trajectory on the Second Output Using Proposed Methods: (a) By GWO and QO – GWO, (b) By GOA and QO – GOA, (c) By AFSA and QO – AFSA, (d) By ABC and QO – ABC, (e) By PSO and QO – PSO.

tuned MPID controller. In this part, a comparison is performed between the conventional method, which is called C-MPID in both figures, the tuned swarm-based

controller, and the QO-SMPID controller. The proposed tracking method is followed for the first obtained output from the MIMO AC/HVDC with ESS model in Figure 16.

It results for the tracking trajectory of the second output with the proposed method, is also presented in Figure 17. By considering these figures, it can be concluded that the proposed QO-SBOAs method for tuning MPID provides well-trackable with high accuracy performance for the test system. According to Figure 11, It should be reminded that the applied MPID model for this simulation is as follows:

$$G_{C1}(s) = k_{p11} + \frac{k_{i11}}{s} + k_{d11}s, G_{C2}(s) = k_{p22} + \frac{k_{i22}}{s} + k_{d22}s \quad (50)$$

The digitized calculated results for the first output (y_1) in the MIMO model are also provided in Table 3.

Table 3 illustrates the digitized obtained results among the implementation of the main scenario. This table can realize more accurate analysis on all selected SBOAs and therefore it presents more detailed data about the proposed MPID controller.

As it is viewed, Table 3 indicates that QOGWO presents a suitable improvement in the tracking process of the reference input in both obtained outputs. Also, the record results in this table confirm the authenticity of the accommodated outcomes in Table 2.

As it was explained, $\Delta P_{tieAC12}$, as an appropriate common state among the simulation process, can be also considered for additional evaluation of the obtained results from the test system. Figure 18, illustrates the variation of this variable among all the employed SBOAs in AC/HVDC with ESS model.

As it is clear that the tie-line AC power deviations ($\Delta P_{tieAC12}$) between areas among employing a step load disturbance will be zero [131] and equation (5) can be rewritten, according to MIMO input as follows:

$$\Delta P_{tieAC12} = K_{com} (\Delta y_1 - \Delta y_2) \quad (51)$$

where $\Delta P_{tieAC12}$ exhibits the tie-line AC power deviations between two areas. According to Figure 18, utilizing the QO-SBOAs in AC/HVDC with ESS model occur that $\Delta P_{tieAC12}$ presents the most closed variations to zero. By attention to this figure, it can be observed that the applied QO-SBOAs provide a higher degree of convergence, compared with the conventional SBOAs

Also, by attention to Table 3, it is considered that QOGWO shows a higher trackability for the first calculated output (Δy_1) from the MIMO test system. Similarly, this fact is repeated for the second obtained output (Δy_2) in comparison with other SBOAs.

C. SENSITIVITY ANALYSIS

According to a standard definition, the capability of a system to execute impressively, when its variables differ among a specific supportable range is called robustness. Therefore,

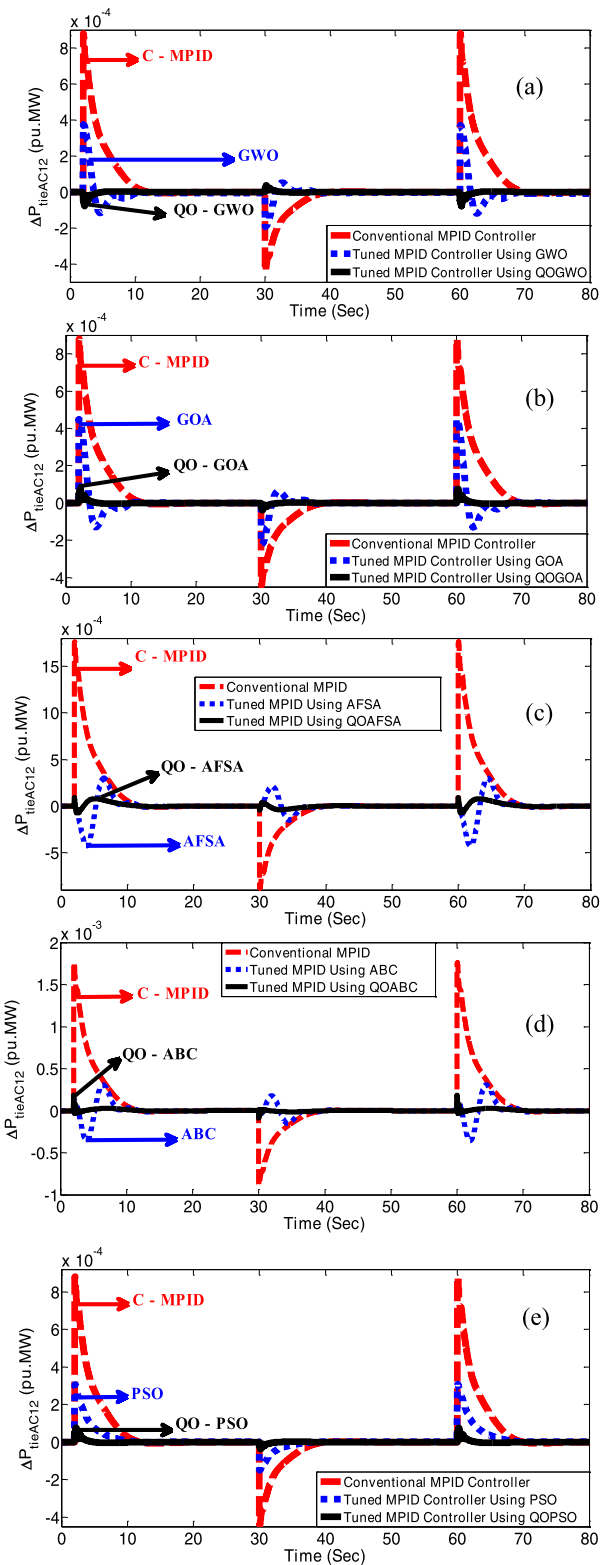


FIGURE 18. The Tie – Line AC Power Deviation among Tracking Trajectory: (a) By GWO and QO – GWO, (b) By GOA and QO – GOA, (c) By AFSA and QO – AFSA, (d) By ABC and QO – ABC, (e) By PSO and QO – PSO.

it is possible to describe the sensitivity analysis as a comparative method for achieving the robustness of the simulated MPID controller by changing the operation loading

TABLE 3. Evaluation of the tracking trajectory performance (for the first input y_1) in the studied scenario using QOSBOAs.

Model Time		Main Scenario – QOSBOAs on Δy_1				
time	Input	QOGO A	QOGWO	QOAFSA	QOABC	QOPSO
t (Sec)	r	Δy_1	Δy_1	Δy_1	Δy_1	Δy_1
3	0.03	0.03197	0.03147	0.03254	0.03183	0.03197
4	0.03	0.03026	0.03012	0.03134	0.0302	0.03026
5	0.03	0.03063	0.03063	0.03152	0.0306	0.03063
6	0.03	0.03142	0.03146	0.03196	0.0314	0.03141
7	0.03	0.03178	0.03185	0.03105	0.03184	0.03179
8	0.03	0.03171	0.03176	0.03079	0.03177	0.0317
9	0.03	0.03134	0.03142	0.03136	0.03143	0.03137
10	0.03	0.03097	0.031	0.03091	0.03102	0.03097
31	0.015	0.014	0.01426	0.01372	0.01408	0.014
32	0.015	0.01487	0.01494	0.01433	0.0149	0.01487
33	0.015	0.01469	0.01469	0.01424	0.0147	0.01469
34	0.015	0.01431	0.01427	0.01452	0.01429	0.0143
35	0.015	0.01411	0.01408	0.01498	0.01408	0.01412
36	0.015	0.01415	0.01422	0.0141	0.01411	0.01415
37	0.015	0.01431	0.01439	0.01432	0.01428	0.01431
38	0.015	0.01451	0.01459	0.01454	0.01449	0.01451
39	0.015	0.0147	0.01479	0.01473	0.01468	0.0147
40	0.015	0.01484	0.01488	0.01486	0.01483	0.01484
61	0.045	0.0472	0.04649	0.04757	0.04684	0.047
62	0.045	0.04526	0.04512	0.04635	0.04521	0.04526
63	0.045	0.04562	0.04562	0.04652	0.04559	0.04562
64	0.045	0.0464	0.04646	0.04636	0.04642	0.0464
65	0.045	0.04671	0.04685	0.04705	0.04683	0.04678
66	0.045	0.0467	0.04677	0.04679	0.04677	0.04673
67	0.045	0.04637	0.04642	0.04636	0.04644	0.04637
68	0.045	0.04597	0.0456	0.04592	0.04602	0.04595
69	0.045	0.04561	0.04563	0.04555	0.04564	0.04651
70	0.045	0.04533	0.04534	0.04527	0.04535	0.04533
Model Time		Main Scenario – QOSBOAs on Δy_2				
time	Input	QOGO A	QOGWO	QOAFSA	QOABC	QOPSO
t (Sec)	r	Δy_2	Δy_2	Δy_2	Δy_2	Δy_2
3	0.03	0.03147	0.03313	0.03197	0.03209	0.03245
4	0.03	0.03012	0.03048	0.03026	0.03014	0.03071
5	0.03	0.03063	0.03009	0.03063	0.0303	0.03109
6	0.03	0.03146	0.03066	0.03141	0.03099	0.03188
7	0.03	0.03185	0.03106	0.03178	0.03134	0.03225
8	0.03	0.03176	0.0311	0.0317	0.03131	0.03218
9	0.03	0.03142	0.03092	0.03137	0.03107	0.03184
10	0.03	0.031	0.03068	0.03097	0.03078	0.03143
31	0.015	0.01426	0.01342	0.014	0.01395	0.01421
32	0.015	0.01494	0.01475	0.01487	0.01493	0.01509
33	0.015	0.01469	0.01496	0.01469	0.01485	0.01491
34	0.015	0.01427	0.01467	0.0143	0.01451	0.01451
35	0.015	0.01408	0.01447	0.01411	0.01433	0.01432
36	0.015	0.01412	0.01445	0.01415	0.01434	0.01436
37	0.015	0.01429	0.01454	0.01431	0.01446	0.01453
38	0.015	0.0145	0.01466	0.01451	0.01461	0.01473
39	0.015	0.01469	0.01477	0.0147	0.01474	0.01492
40	0.015	0.01483	0.01486	0.01484	0.01484	0.01506
61	0.045	0.04649	0.04815	0.047	0.04711	0.04771
62	0.045	0.04512	0.04549	0.04526	0.04515	0.04594
63	0.045	0.04562	0.04509	0.04562	0.04529	0.0463
64	0.045	0.04646	0.04566	0.0464	0.04598	0.0471
65	0.045	0.04685	0.04606	0.04678	0.04634	0.04748
66	0.045	0.04677	0.0461	0.0467	0.04631	0.0474
67	0.045	0.04642	0.04592	0.04637	0.04607	0.04707
68	0.045	0.046	0.04568	0.04597	0.04578	0.04666
69	0.045	0.04563	0.04546	0.04561	0.04552	0.04629
70	0.045	0.04534	0.04529	0.04533	0.04532	0.04601

situation and the test system factors. Following the nature of AC/HVDC system with ESS model, as it was explained in (3) and Figure 2, there are two effective parameters in the

structure of the test system which are proportioned to the power deviation from ESS in each area, J_{em1} and J_{em2} . So, the range of $\pm 50\%$ with steps of $\%25$ in the gain of the inertia

emulators, (J_{emi}), is considered for performing the sensitivity analysis in this Section.

The obtained results from QO-SBOAs are investigated by considering the new applied conditions. The optimized MPID controller coefficients, final minimum objective value, and its terms, containing SI, ST, and RT, based on the deviation of the selected parameters, are presented in Table 4.

In this table, it is observed that the test system efficiency changes from its nominal tunings. Table 4 is concentrated to show the variation of the optimization process components by considering the variation of J_{em1} and J_{em2} . It is notable in this table that the objective value and its components for AC/HVDC with ESS model parameter variations are among the tolerable limitation and closed equal to the obtained results at the nominal condition. Therefore, it can be derived from Table 4 that the proposed MPID controller, tuned through QO-SBOAs, is robust enough to be employed under various uncertain situations. To endure the tolerable effectiveness of variations in the MIMO test system, the tie-line AC power deviations between areas, $\Delta P_{tieAC12}$, is considered among the tuning MPID controller using QOGWO for both scenarios in Figure 19. As it is observed from this figure, the obtained simulation results satisfy the record data in Table 4.

D. COMPARISON: THE PROPOSED OBJECTIVE FUNCTION WITH THE STANDARD TYPE

In this section, it is necessary to select a specified approach among the optimization process using QO-SBOAs. By attention to the determined features of step response and its accessibility in every iteration of the simulation, different fitness functions are used for that purpose [132]. But in this work, three performance indices are considered: Integral of Time multiplied by Absolute Error (ITAE), Integral of Absolute Error (IAE), and Integral of Time multiplied by the Squared Error (ITSE). These performance indices are defined by equation (52), where frequency deviation in area 1 and 2 ($\Delta\omega_1$ and $\Delta\omega_2$) also $\Delta P_{tie-AC12}$ will be calculated in the time domain.

$$\begin{cases} IAE(Z) = \int_0^{T_{final}} ((\Delta\omega_1) + (\Delta\omega_2) + (\Delta P_{tie-AC12})) \\ ITAE(Z) = \int_0^{T_{final}} t((\Delta\omega_1) + (\Delta\omega_2) + (\Delta P_{tie-AC12})) \\ ITSE(Z) = \int_0^{T_{final}} t((\Delta\omega_1)^2 + (\Delta\omega_2)^2 + (\Delta P_{tie-AC12})^2) \end{cases} \quad (52)$$

where T_{final} is the final simulation time. Therefore, the tuning MPID process is accomplished based on the standard fitness function from (52).

Figure 19, is shown as well the effectiveness of the designed QO-SBOAs through the proposed fitness function base on the step response features in comparison with the standard objective functions, as defined in (52). For achieving more simplicity in simulation, by considering all the same situations, the tuning MPID controller process is done by

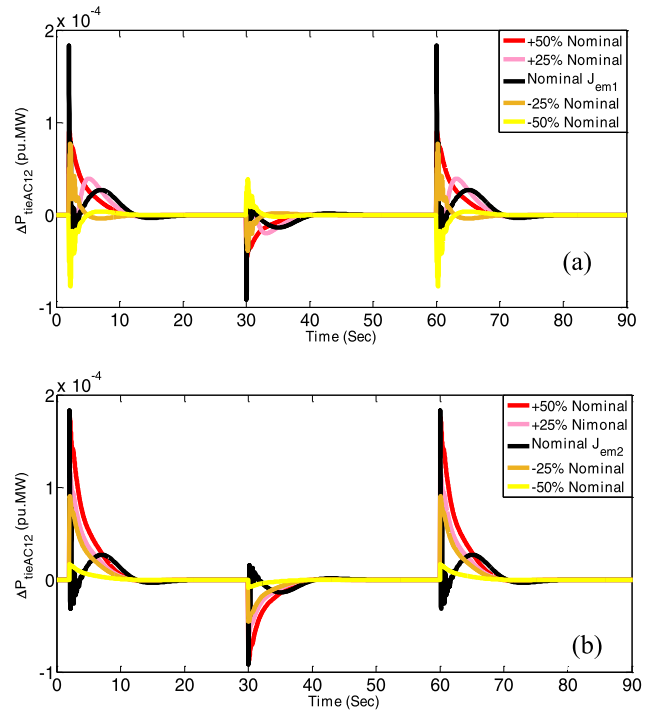


FIGURE 19. The Tie - Line AC power deviation among sensitivity analysis: (a) J_{em1} deviation, (b) J_{em2} deviation.

QOGWO, as the most suitable SBOAs for the optimization process using three standard fitness functions, which were introduced in (52), and then, by Figure 20, the obtained simulation results are compared with the proposed objective function. In this comparison, the variation of reference input, for the main scenarios, the calculated output signal from the MIMO system, and their differences are presented and analyzed in this figure.

According to Figure 20, it is observed that the proposed objective function, which is defined based on the step response features of the test system, can present a higher trackability and more suitable accuracy than all three standard fitness functions, such as IAE, ITSE, and ITAE. Therefore, it can be concluded that the proposed objective function not only can compete with the conventional standard methods but also it can pass them in most of the simulation time impressively.

X. FUTURISTIC OPEN QUESTIONS

To accelerate enhancing the appearance trajectory of swarm-based optimization algorithms (SBOAs), this work, by itself can't cover all open questions that should be investigated in the forthcoming years also occurred. Furthermore, recently researches can introduce higher developed and well-performance learning methods in comparison with quasi-oppositional (QO) strategy. Therefore, considering different vibrates in this research area, the authors certainly specify a futuristic room for modification.

Moreover, the implementation of the proposed objective function, based on the step response from a multi-input

TABLE 4. Sensitivity analysis of MIMO AC/HVDC with ESS model.

QO-SBOAs		Tuned MPID Coefficients						Objective Value	Z		
QOGWO		K_{p11}	K_{p22}	K_{i11}	K_{i22}	K_{d11}	K_{d22}	SI	ST	RT	
J_{em1}	+ 50%	1.2271	-0.0961	0.1851	-0.0436	-0.3299	0.1587	756.105	63.0087	504.07	189.0263
	+ 25%	1.1979	-0.0938	0.1807	-0.0425	-0.3221	0.1549	738.1025	61.5085	492.0684	184.5256
	Nominal	1.1687	-0.0915	0.1763	-0.0415	-0.3142	0.1511	720.1	60.0083	480.0667	180.025
	- 25%	1.1103	-0.0869	0.1675	-0.0394	-0.2985	0.1435	684.095	57.0079	456.0634	171.0238
	- 50%	1.081	-0.0846	0.1631	-0.0384	-0.2906	0.1398	666.0925	55.5077	444.0617	166.5231
QOGO											
J_{em1}	+ 50%	1.2881	-0.0961	0.1509	-0.4659	-0.1559	-0.3450	782.355	65.1963	521.57	195.5888
	+ 25%	1.2575	-0.0938	0.1473	-0.4548	-0.1522	-0.3368	763.7275	63.644	509.1516	190.9319
	Nominal	1.2268	-0.0915	0.1437	-0.4437	-0.1485	-0.3286	745.1	62.0917	496.7333	186.275
	- 25%	1.1655	-0.0869	0.1365	-0.4215	-0.1411	-0.3122	707.845	58.9871	471.8966	176.9613
	- 50%	1.1348	-0.0846	0.1329	-0.4104	-0.1374	-0.3040	689.2175	57.4348	459.4783	172.3044
QOAFSA											
J_{em1}	+ 50%	1.2184	-0.0961	0.1918	0.1038	0.624	0.8383	756.42	63.035	504.28	189.105
	+ 25%	1.1894	-0.0938	0.1873	0.1014	0.6092	0.8184	738.41	61.5341	492.2734	184.6025
	Nominal	1.1604	-0.0915	0.1827	0.0989	0.5943	0.7984	720.4	60.0333	480.2667	180.1
	- 25%	1.1024	-0.0869	0.1736	0.094	0.5646	0.7585	684.38	57.0316	456.2534	171.095
	- 50%	1.0734	-0.0846	0.169	0.0915	0.5497	0.7385	666.37	55.9871	444.0617	166.5231
QOPSO											
J_{em1}	+ 50%	1.278	-0.0961	0.1473	-0.1242	-0.1254	0.3147	787.605	65.6337	525.07	196.9013
	+ 25%	1.2475	-0.0938	0.1438	-0.1213	-0.1224	0.3072	768.8525	64.071	512.5684	192.2131
	Nominal	1.2171	-0.0915	0.1403	-0.1183	-0.1194	0.2997	750.1	62.5083	500.0667	187.525
	- 25%	1.1562	-0.0869	0.1333	-0.1124	-0.1134	0.2847	712.595	59.3829	475.0634	178.1488
	- 50%	1.1258	-0.0846	0.1298	-0.1094	-0.1104	0.2772	693.8425	57.8202	462.5617	173.4606
QOABC											
J_{em1}	+ 50%	1.2209	-0.0961	0.1788	0.0957	0.2399	0.2253	768.18	64.015	512.12	192.045
	+ 25%	1.1919	-0.0938	0.1746	0.0934	0.2342	0.22	749.89	62.4909	499.9266	187.4725
	Nominal	1.1628	-0.0915	0.1703	0.0911	0.2285	0.2146	731.6	60.9667	487.7333	182.9
	- 25%	1.1047	-0.0869	0.1618	0.0865	0.2171	0.2039	695.02	57.9184	463.3466	173.755
	- 50%	1.0756	-0.0846	0.1575	0.0843	0.2114	0.1985	676.73	56.3942	451.1533	169.1825
QOGWO											
J_{em2}	+ 50%	1.2564	-0.0984	0.1895	-0.0446	-0.3378	0.1624	774.1075	64.5089	516.0717	193.5269
	+ 25%	1.2096	-0.0947	0.1825	-0.043	-0.3252	0.1564	745.3035	62.1086	496.869	186.3259
	Nominal	1.1687	-0.0915	0.1763	-0.0415	-0.3142	0.1511	720.1	60.0083	480.0667	180.025
	- 25%	1.1395	-0.0892	0.1719	-0.0405	-0.3063	0.1473	702.0975	58.5081	468.065	175.5244
	- 50%	1.0927	-0.0856	0.1648	-0.0388	-0.2938	0.1413	673.2935	56.1078	448.8624	168.3234
QOGO											
J_{em2}	+ 50%	1.3188	-0.0984	0.1545	-0.477	-0.1596	-0.3532	800.9825	66.7486	533.9883	200.2456
	+ 25%	1.2697	-0.0947	0.1487	-0.4592	-0.1537	-0.3401	771.1785	64.2649	514.119	192.7946
	Nominal	1.2268	-0.0915	0.1437	-0.4437	-0.1485	-0.3286	745.1	62.0917	496.7333	186.275
	- 25%	1.1961	-0.0892	0.1401	-0.4326	-0.1448	-0.3204	726.4725	60.5394	484.315	181.6181
	- 50%	1.1471	-0.0856	0.1344	-0.4149	-0.1388	-0.3072	696.6685	58.0557	464.4456	174.1671
QOAFSA											
J_{em2}	+ 50%	1.2474	-0.0984	0.1964	0.1063	0.6389	0.8583	774.43	64.5358	516.2867	193.6075
	+ 25%	1.201	-0.0947	0.1891	0.1024	0.6151	0.8263	745.614	62.1345	497.076	186.4035
	Nominal	1.1604	-0.0915	0.1827	0.0989	0.5943	0.7984	720.4	60.0333	480.2667	180.1
	- 25%	1.1314	-0.0892	0.1781	0.0964	0.5794	0.7784	702.39	58.5325	468.26	175.5975
	- 50%	1.085	-0.0856	0.1708	0.0925	0.5557	0.7465	673.574	56.1311	449.0494	168.3935
QOPSO											
J_{em2}	+ 50%	1.3084	-0.0984	0.1508	-0.1272	-0.1284	0.3222	806.3575	67.1964	537.5717	201.5894
	+ 25%	1.2597	-0.0947	0.1452	-0.1224	-0.1236	0.3102	776.3535	64.6961	517.569	194.0884
	Nominal	1.2171	-0.0915	0.1403	-0.1183	-0.1194	0.2997	750.1	62.5083	500.0667	187.525
	- 25%	1.1867	-0.0892	0.1368	-0.1153	-0.1164	0.2922	731.3475	60.9456	487.565	182.8369
	- 50%	1.138	-0.0856	0.1312	-0.1106	-0.1116	0.2802	701.3435	58.4453	467.5624	175.3359
QOABC											
J_{em2}	+ 50%	1.25	-0.0984	0.1831	0.0979	0.2456	0.2307	786.47	65.5392	524.3133	196.6175
	+ 25%	1.2035	-0.0947	0.1763	0.0943	0.2365	0.2221	757.206	63.1005	504.804	189.3015
	Nominal	1.1628	-0.0915	0.1703	0.0911	0.2285	0.2146	731.6	60.9667	487.7333	182.9
	- 25%	1.1337	-0.0892	0.166	0.0888	0.2228	0.2092	713.31	59.4425	475.54	178.3275
	- 50%	1.0872	-0.0856	0.1592	0.0852	0.2136	0.2007	684.046	57.0039	456.0306	171.0115

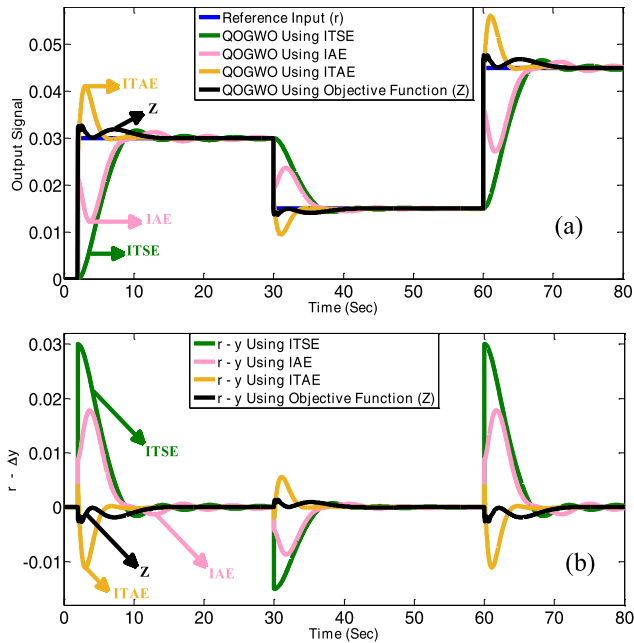


FIGURE 20. The performance comparison between the proposed objective function and the three standard fitness functions: (a) The obtained outputs, (b) Difference between r and outputs.

multi-output (MIMO) transfer function, and comparison with the standard fitness functions such as IAE, ITSE, and ITAE is evaluated on an AC/HVDC with ESS mode as a 2×2 input-output system. It is expected that the proposed performance index will be encountered with a new challenge for a higher degree MIMO model. Hereupon, with attention to this point, the authors define a specified room for future adjustments in this investigation field.

XI. CONCLUSION

In this study, an endeavor is constructed to enhance tracking control strategy on a test AGC interconnected system with Virtual inertia based HVDC model employing a tuned MPID controller in which the matrix of its coefficients is set based on the selected SBOAs that they are provided with utilizing an effective nature-inspired optimization methodology, called quasi-oppositional based learning (QO-BL) algorithm. Growing greeted from QO-BL in recent years on different fields of power system including optimal allocation and optimal load dispatch and LFC also the applied ever-increasing modifications for QO-BL method, because of its high capability to pass the local minima problem among the optimization process, encouraged the authors to utilize this technique for the paper.

Multivariable proportional – integral – derivative (MPID) controller, as the most flexible solution in various real-world control problems, is defined as a multi-input multi-output (MIMO) model. Similar to conventional PID controller, the behavior of all transient and steady-state conditions is covered through three impressive coefficients, containing K_P , K_I , and K_D , that they appear as three individual functional

matrices. The advantages of the necessity of the MPI controller utilization are such as: (i) its feasibility and ease to be implemented. (ii) to be well-trusted and high-citations in all scientific societies. Therefore, a tuning MPID controller method is presented in this work for achieving a flexible output tracking strategy. Moreover, the recent finding of various and impressive features of swarm-based optimization algorithms (SBOAs), such as high-level rapidity and convergence power, has persuaded scientists and researchers into applying them for solving complex problems in many different fields.

Grasshoppers Optimization Algorithm (GOA), Grey Wolf Optimization (GWO), Artificial Fish Swarm Algorithm (AFSA), Artificial Bee Colony (ABC), and Particle Swarm Optimization (PSO) as the most important and the newest SBOAs, are selected in this work. For achieving the best possible evaluation, different analyses according to the step load deviations are selected as the reference inputs. The tuning progress of swarm-based multivariable PID (SMPID) controller using QO method is upgraded for finding the optimized coefficients k_{ij} , ($i = 1, 2, \dots, 6$), while the obtained output MIMO system is tracking the assumed scenarios preciously. After that, a comprehensive evaluation is achieved on the tuned SMPID controller by QO strategy in comparison with the conventional MPID (C-MPID) controller design.

Another section was also presented to assess the effectiveness of the proposed objective function, based on step response characteristics of the MIMO test system, which was utilized in our previous papers for tuning MPI controller, in comparison with the standard fitness functions such as IAE, ITSE, and ITAE. Therefore, in similar conditions, the calculated simulation results using QOGWO, as the highest degree of trackability than all QO-SBOAs, are compared with the obtained resembling outcomes through three standard cost functions. According to this comparison, it is viewed that the proposed objective function provides higher flexibility in both scenarios in comparison with the typical fitness functions.

It should be noted that the robustness of the designed controller is achieved by sensitivity analysis of the simulation results according to change two impressive parameters in AC/HVDC with ESS model, J_{em1} and J_{em2} proportion to each area. This study indicates that despite the implementation of sensitive changes in the tuning process of SMPID controller, the obtained outputs can track the reference input for both scenarios suitably and accurately.

FULL INDEX TERMS

- Artificial Bee Colony (ABC)
- Artificial Fish Swarm Algorithm (AFSA)
- Automatic Generation Control (AGC)
- Conventional Multivariable PID (C - MPID)
- Energy Storage System (ESS)
- Generation Units (GENs)
- Grasshoppers Optimization Algorithm (GOA)

Grey Wolf Optimization	(GWO)		
Integral Absolute Error	(IAE)		
Integral Time multiple Absolute Error	(ITAE)		
Integral Time multiple Squared Error	(ITSE)		
Multi-Input Multi-Output	(MIMO)		
Multivariable proportional – integral – derivative	(MPID)		
Number of Relevant Papers	(NORP)		
Opposite – Based Learning	(OBL)		
Particle Swarm Optimization	(PSO)		
Quasi Oppositional – Based Learning	(QO - BL)		
Quasi Oppositional – Based ABC	(QO - ABC)		
Quasi Oppositional – Based AFSA	(QO - AFSA)		
Quasi Oppositional – Based GOA	(QO - GOA)		
Quasi Oppositional – Based GWO	(QO - GWO)		
Quasi Oppositional – Based PSO	(QO - PSO)		
Quasi Oppositional – Based SBOAs	(QO - SBOAs)		
Rate of Change of Frequency	(ROCOF)		
Swarm – Based Optimization Algorithms	(SBOAs)		
Stability Index	(SI)		
Swarm – Based MPID	(SMPID)		
Settling Time	(ST)		
Rise Time	(RT)		
CONSTANTS			
K_α	Inertial Proportional Conversion Gain		
ω_0	Nominal Frequency		
K_{pi}	The Model Gain for Total Active Power in i^{th} area		
T_{pi}	The Time Constant for Total Active Power in i^{th} area		
J_{emi}	The Emulated Inertia for ESS Model in i^{th} area		
β_i	The Frequency Bias in i^{th} area		
K_i, K_k	The Proportional Coefficients for $\Delta\omega_i$ and $\Delta\omega_k$		
$A_{(12 \times 12)}^{\text{ESS}}$	State Matrix for AC/HVDC with ESS Steady State Model		
$B_{(12 \times 2)}^{\text{ESS}}$	Input Matrix for AC/HVDC with ESS Steady State Model		
$C_{(2 \times 12)}^{\text{ESS}}$	Output Matrix for AC/HVDC with ESS Steady State Model		
A_{Plant}	State Matrix for the Plant Model		
B_{Plant}	Input Matrix for the Plant Model		
E_{W}	State Matrix for the Exogenous Model		
C_{Plant}^y	Output Matrix for the Plant Model		
D_{Plant}^{yu}	Distribution Matrix for the Plant Model		
D_{Plant}^{yw}	Distribution Matrix for the Exogenous Model		
C_{Plant}^e	State Matrix for the Error Model		
D_{Plant}^{eu}	Distribution Matrix for the Error Model		
f	The intensity of Absorption Constant for GOA		
l	Attractive Length Scale Constant for GOA		
c	Comfort Zone Constant for GOA		
J_r	Jumping Rate in QO Method		
VARIABLES			
$\Delta P_{\text{emulate}}$	The Power Reference Deviation		
$\Delta\omega_i$	The Frequency Deviation in i^{th} area		
ΔP_{mi}	Total Active Power from GENs within area i and k		
$\Delta P_{\text{ESS}i}$	The Power Variation for Emulating Inertia within area i and k		
$\Delta P_{\text{tieAC}12}$	The Tie-Line AC Power Deviation Between Areas		
Δx_{ESS}	The State Variables for AC/HVDC with ESS Model		
Δu_{ESS}	The Input Variables for AC/HVDC with ESS Model		
Δy_{ESS}	The Output Variables for AC/HVDC with ESS Model		
$G_{\text{Tf}}^{\text{ESS}}$	Transfer Function for AC/HVDC with ESS Model		
X_{Plant}	The State Variables for Plant Model		
Y_{Plant}	The Output Variables for Plant Model		
E_{Plant}	The Error Variables for Plant Model		
W_{Plant}	The State Variables for Exogenous Model		
x_i^0	Opposite Number		
x_i^{q0}	Quas - Opposite Number		
SI	Stability Index		
RT	Rise Time Index		
ST	Settling Time Index		
Z	The Proposed Objective Function		
r	Reference Input		
Δy_1	The Obtained First Output from The Test System		
Δy_2	The Obtained Second Output from The Test System		
$\Delta P_{\text{ithS}/\text{tieAC}12}$	The Tie-Line AC Power Deviation Between Areas for i^{th} Scenario		
Δy_1^{ithS}	The Obtained First Output from The Test System in i^{th} Scenario		
Δy_2^{ithS}	The Obtained Second Output from The Test System in i^{th} Scenario		
REFERENCES			
[1]	P. Tielens and D. Van Hertem, "The relevance of inertia in power systems," <i>Renew. Sustain. Energy Rev.</i> , vol. 55, Mar. 2016, pp. 999–1009.		
[2]	P. Kundur, <i>Power System Stability and Control</i> . New York, NY, USA: McGraw-Hill, 1994.		
[3]	H. Saadat, <i>Power System Analysis</i> . New York, NY, USA: McGraw-Hill, 1999.		
[4]	Z. E. Al-Haiki and A. N. Shaikh-Nasser, "Power transmission to distant offshore facilities," <i>IEEE Trans. Ind. Appl.</i> , vol. 47, no. 3, pp. 1180–1183, May 2011.		
[5]	W. Wang, L. Jiang, Y. Cao, and Y. Li, "A parameter alternating VSG controller of VSC-MTDC systems for low frequency oscillation damping," <i>IEEE Trans. Power Syst.</i> , vol. 35, no. 6, pp. 4609–4621, May 2020.		
[6]	C. Du, E. Agneholm, and G. Olsson, "Use of VSC-HVDC for industrial systems having onsite generation with frequency control," <i>IEEE Trans. Power Del.</i> , vol. 23, no. 4, pp. 2233–2240, Oct. 2008.		
[7]	Y. Li, Z. Zhang, Y. Yang, Y. Li, H. Chen, and Z. Xu, "Coordinated control of wind farm and VSC-HVDC system using capacitor energy and kinetic energy to improve inertia level of power systems," <i>Int. J. Electr. Power Energy Syst.</i> , vol. 59, pp. 79–92, Jul. 2014.		

- [8] L. Zhang, L. Harnefors, and H.-P. Nee, "Power-synchronization control of grid-connected voltage-source converters," *IEEE Trans. Power Syst.*, vol. 25, no. 2, pp. 809–820, May 2010.
- [9] P. Rodriguez, I. Candela, C. Citro, J. Rocabert, and A. Luna, "Control of grid-connected power converters based on a virtual admittance control loop," in *Proc. 15th Eur. Conf. Power Electron. Appl. (EPE)*, 2013, pp. 1–10.
- [10] L. D. S. Coelho and M. W. Pessôa, "A tuning strategy for multivariable PI and PID controllers using differential evolution combined with chaotic Zaslavskii map," *Expert Syst. Appl.*, vol. 38, no. 11, pp. 13694–13701, Oct. 2011.
- [11] K. H. Ang, G. Chong, and Y. Li, "PID control system analysis, design, and technology," *IEEE Trans. Control Syst. Technol.*, vol. 13, no. 4, pp. 559–576, Jul. 2005.
- [12] A. Marin, J. A. Hernandez R, and J. A. Jimenez, "Tuning multivariable optimal PID controller for a continuous stirred tank reactor using an evolutionary algorithm," *IEEE Latin Amer. Trans.*, vol. 16, no. 2, pp. 422–427, Feb. 2018, doi: [10.1109/TLA.2018.8327395](https://doi.org/10.1109/TLA.2018.8327395).
- [13] M. W. Iruthayarajan, S. G. Prasad, S. Abishek, and P. Vignesh, "Chaotic GSA based design of multivariable centralised fractional-order PID controller for TRMS," in *Proc. Global Conf. Advancement Technol. (GCAT)*, Bangalore, India, Oct. 2019, pp. 1–4, doi: [10.1109/GCAT47503.2019.8978462](https://doi.org/10.1109/GCAT47503.2019.8978462).
- [14] K. Lakshmi, T. Rajesh, D. Anusuya, G. Prowince P., and B. Pranesh, "Design and implementation of multivariable quadruple tank system with different PID tuning control techniques," in *Proc. Int. Conf. Adv. Comput. Commun. Eng. (ICACCE)*, Sathyamangalam, India, Apr. 2019, pp. 1–6, doi: [10.1109/ICACCE46606.2019.9079983](https://doi.org/10.1109/ICACCE46606.2019.9079983).
- [15] N. Hanani, F. Syazwanadira, N. A. Fakharulrazi, F. Yakub, Z. A. Rasid, and S. Sarip, "Full control of quadrotor unmanned aerial vehicle using multivariable proportional integral derivative controller," in *Proc. IEEE 9th Int. Conf. Syst. Eng. Technol. (ICSET)*, Shah Alam, Malaysia, Oct. 2019, pp. 447–452, doi: [10.1109/ICSEngT.2019.8906418](https://doi.org/10.1109/ICSEngT.2019.8906418).
- [16] W. K. Ho, T. H. Lee, and O. P. Gan, "Tuning of multiloop proportional-integral-derivative controllers based on gain and phase margin specifications," *Ind. Eng. Chem. Res.*, vol. 36, no. 6, pp. 2231–2238, 1997.
- [17] V. V. Kumar, V. S. R. Rao, and M. Chidambaram, "Centralized PI controllers for interacting multivariable processes by synthesis method," *ISA Trans.*, vol. 51, no. 3, pp. 400–409, May 2012.
- [18] J. K. L. N. Sarma and M. Chidambaram, "Centralized PI/PID controllers for nonsquare systems with RHP zeros," *Indian Inst. Sci.*, vol. 85, no. 4, pp. 201–214, 2005.
- [19] A. Montazar, P. J. Van Overloop, and R. Brouwer, "Centralized controller for the Narmada main canal," *Irrigation Drainage*, vol. 54, no. 1, pp. 79–89, 2005.
- [20] F. Morilla, F. Vazquez, and J. Garrido, "Centralized PID control by decoupling for TITO processes," in *Proc. IEEE Int. Conf. Emerg. Technol. Factory Autom.*, Sep. 2008, pp. 1318–1325.
- [21] J. Garrido, F. Morilla, and F. Vazquez, "Centralized PID control by decoupling of a boiler-turbine unit," in *Proc. Eur. Control Conf. (ECC)*, Budapest, Hungary, Aug. 2009, pp. 4007–4012.
- [22] M. Willjuice Iruthayarajan and S. Baskar, "Covariance matrix adaptation evolution strategy based design of centralized PID controller," *Expert Syst. Appl.*, vol. 37, no. 8, pp. 5775–5781, Aug. 2010.
- [23] A. A. El-Sulaiman, Z. Elrazaz, and M. Barakat, "Impact of power system stabilizer installation on steady state stability performance," *J. King Saud Univ.-Eng. Sci.*, vol. 2, no. 1, pp. 43–51, 1990.
- [24] H. Liu, J. Su, Y. Yang, Z. Qin, and C. Li, "Compatible decentralized control of AVR and PSS for improving power system stability," *IEEE Syst. J.*, early access, Jun. 29, 2020, doi: [10.1109/JSYST.2020.3001429](https://doi.org/10.1109/JSYST.2020.3001429).
- [25] A. Kahouli, T. Guesmi, H. H. Abdallah, and A. Ouali, "A genetic algorithm PSS and AVR controller for electrical power system stability," in *Proc. 6th Int. Multi-Conf. Syst., Signals Devices*, 2009, pp. 1–6.
- [26] B. Selvalala and D. Devaraj, "Co-ordinated design of AVR-PSS using multi-objective genetic algorithm," in *Swarm, Evolutionary, and Memetic Computing*. Berlin, Germany: Springer, 2010, pp. 481–493.
- [27] H. J. Blakelock, *Automatic Control of Aircraft and Missiles*. Hoboken, NJ, USA: Wiley, Jan. 1991.
- [28] W.-S. Yu, "Design of a power system stabilizer using decentralized adaptive model following tracking control approach," *Int. J. Numer. Model., Electron. Netw., Devices Fields*, vol. 23, no. 2, pp. 63–87, Jan. 2009, doi: [10.1002/jnm.722](https://doi.org/10.1002/jnm.722).
- [29] K. B. Meziane and I. Boumhidi, "Optimized type-2 fuzzy logic PSS Combined with H_∞ tracking control for the multi-machine power system," in *Embedded Systems and Artificial Intelligence (Advances in Intelligent Systems and Computing)*, vol. 1076. Singapore: Springer, 2020, pp. 193–204.
- [30] F. Dib, K. B. Meziane, and I. Boumhidi, "Robust H_∞ tracking control combined with optimized PSS by PSO algorithm for multi-machine power system," *J. Elect. Syst.*, vol. 11, pp. 36–48, Dec. 2014.
- [31] J. C. Gamazo-Real, E. Vázquez-Sánchez, and J. Gómez-Gil, "Position and speed control of brushless DC motors using sensorless techniques and application trends," *Sensors*, vol. 10, no. 7, pp. 6901–6947, Jul. 2010, doi: [10.3390/s100706901](https://doi.org/10.3390/s100706901).
- [32] C. B. Regaya, A. Zaafour, and A. Chaari, "Electric drive control with rotor resistance and rotor speed observers based on fuzzy logic," *Math. Problems Eng.*, vol. 2014, Feb. 2014, Art. no. 207826.
- [33] A. Zaafour, F. Farhani, and A. Chaari, "Robust observer design with pole placement constraints for induction motor control," *Elektron Elektrotech*, vol. 21, no. 1, pp. 18–22, Apr. 2015.
- [34] H. Kwakernaak and R. Sivan, *Linear Optimal Control Systems*. New York, NY, USA: Wiley, 1972.
- [35] Z.-K. Feng, S. Liu, W.-J. Niu, Y. Liu, B. Luo, S.-M. Miao, and S. Wang, "Optimal operation of hydropower system by improved grey wolf optimizer based on elite mutation and quasi-oppositional learning," *IEEE Access*, vol. 7, pp. 155513–155529, 2019.
- [36] D. Guha, P. K. Roy, S. Banerjee, S. Padmanaban, F. Blaabjerg, and D. Chittathuru, "Small-signal stability analysis of hybrid power system with quasi-oppositional sine cosine algorithm optimized fractional order PID controller," *IEEE Access*, vol. 8, pp. 155971–155986, 2020.
- [37] D. Guha, P. K. Roy, and S. Banerjee, "Load frequency control of large scale power system using quasi-oppositional grey wolf optimization algorithm," *Eng. Sci. Technol., Int. J.*, vol. 19, no. 4, pp. 1693–1713, Dec. 2016.
- [38] C. K. Shiva and V. Mukherjee, "A novel quasi-oppositional harmony search algorithm for automatic generation control of power system," *Appl. Soft Comput.*, vol. 35, pp. 749–765, Oct. 2015.
- [39] C. K. Shiva, G. Shankar, and V. Mukherjee, "Automatic generation control of power system using a novel quasi-oppositional harmony search algorithm," *Int. J. Electr. Power Energy Syst.*, vol. 73, pp. 787–804, Dec. 2015.
- [40] M. Nandi, C. K. Shiva, and V. Mukherjee, "TCSC based automatic generation control of deregulated power system using quasi-oppositional harmony search algorithm," *Eng. Sci. Technol., Int. J.*, vol. 20, no. 4, pp. 1380–1395, Aug. 2017.
- [41] S. Dutta, S. Paul, and P. K. Roy, "Optimal allocation of SVC and TCSC using quasi-oppositional chemical reaction optimization for solving multi-objective ORPD problem," *J. Electr. Syst. Inf. Technol.*, vol. 5, no. 1, pp. 83–98, May 2018.
- [42] K. H. Truong, P. Nallagownden, I. Elamvazuthi, and D. N. Vo, "A quasi-oppositional-chaotic symbiotic organisms search algorithm for optimal allocation of DG in radial distribution networks," *Appl. Soft Comput.*, vol. 88, Mar. 2020, Art. no. 106067.
- [43] P. K. Roy and S. Bhui, "Multi-objective quasi-oppositional teaching learning based optimization for economic emission load dispatch problem," *Int. J. Electr. Power Energy Syst.*, vol. 53, pp. 937–948, Dec. 2013.
- [44] W. Warid, H. Hizam, N. Mariun, and N. I. A. Wahab, "A novel quasi-oppositional modified jaya algorithm for multi-objective optimal power flow solution," *Appl. Soft Comput.*, vol. 65, pp. 360–373, Apr. 2018.
- [45] M. A. El-Shorbagy and A. M. El-Refaey, "Hybridization of grasshopper optimization algorithm with genetic algorithm for solving system of non-linear equations," *IEEE Access*, vol. 8, pp. 220944–220961, 2020.
- [46] M. W. Guo, J. S. Wang, L. F. Zhu, S. S. Guo, and W. Xie, "An improved grey wolf optimizer based on tracking and seeking modes to solve function optimization problems," *IEEE Access*, vol. 8, pp. 69861–69893, 2020.
- [47] M. Neshat, G. Sepidnam, M. Sargolzaei, and A. N. Toosi, "Artificial fish swarm algorithm: A survey of the state-of-the-art, hybridization, combinatorial and indicative applications," *Artif. Intell. Rev.*, vol. 42, no. 4, pp. 965–997, Dec. 2014.
- [48] D. Karaboga, "An idea based on honey bee swarm for numerical optimization," Dept. Comput. Eng., Erciyes Univ., Kayseri, Turkey, Tech. Rep. TR06, 2005.
- [49] Y. Zhang, S. Wang, and G. Ji, "A comprehensive survey on particle swarm optimization algorithm and its applications," *Math. Problems Eng.*, vol. 2015, Oct. 2015, Art. no. 931256.

- [50] I. M. H. Naveh, E. Rakhshani, H. Mehrjerdi, J. R. Torres, and P. Palensky, "Design of multivariable PI controller using evolutionary algorithms for VSP based AC/DC interconnected systems," in *Proc. 2nd Int. Conf. Smart Grid Renew. Energy (SGRE)*, Nov. 2019, pp. 1–6.
- [51] E. Rakhshani, I. M. H. Naveh, and H. Mehrjerdi, "Comparative study of SBOAs on the tuning procedure of the designed SMPI controller for MIMO VSP/HVDC interconnected model," *Int. J. Electr. Power Energy Syst.*, vol. 129, Jul. 2021, Art. no. 106812.
- [52] E. Rakhshani, D. Remon, A. M. Cantarellas, and P. Rodriguez, "Analysis of derivative control based virtual inertia in multi-area high-voltage direct current interconnected power systems," *IET Gener., Transmiss. Distrib.*, vol. 10, no. 6, pp. 1458–1469, Apr. 2016.
- [53] K. Pan, A. Teixeira, C. D. Lopez, and P. Palensky, "Co-simulation for cyber security analysis: Data attacks against energy management system," in *Proc. IEEE Int. Conf. Smart Grid Commun. (SmartGridComm)*, Oct. 2017, pp. 253–258.
- [54] E. Rakhshani and P. Rodriguez, "Inertia emulation in AC/DC interconnected power systems using derivative technique considering frequency measurement effects," *IEEE Trans. Power Syst.*, vol. 32, no. 5, pp. 3338–3351, Sep. 2017.
- [55] T. L. Gruyitch, *Tracking Control of Linear Systems*. Boca Raton, FL, USA: CRC Press, 2013.
- [56] M. Fliess, J. Lévine, P. Martin, and P. Rouchon, "Flatness and defect of non-linear systems: Introductory theory and examples," *Int. J. Control*, vol. 61, no. 6, pp. 1327–1361, Jun. 1995.
- [57] M. Fliess, J. Levine, P. Martin, and P. Rouchon, "A lie-backlund approach to equivalence and flatness of nonlinear systems," *IEEE Trans. Autom. Control*, vol. 44, no. 5, pp. 922–937, May 1999.
- [58] A. Saberi, A. A. Stoorvogel, and P. Sannuti, *Control of Linear Systems With Regulation and Input Constraints*. Springer, 2012.
- [59] M. Belal, J. Gaber, H. El-Sayed, and A. Almojel, "Swarm intelligence," in *Handbook of Bioinspired Algorithms and Applications* (CRC Computer & Information Science), vol. 7. London, U.K.: Chapman & Hall, 2006.
- [60] R. Eberhart and J. Kennedy, "A new optimizer using particle swarm theory," in *Proc. 6th Symp. Micro*, 1995, pp. 29–43.
- [61] Y. Meraihi, A. B. Gabis, S. Mirjalili, and A. Ramdane-Cherif, "Grasshopper optimization algorithm: Theory, variants, and applications," *IEEE Access*, vol. 9, pp. 50001–50024, 2021.
- [62] J. Rajpurohit, T. K. Sharma, A. Abraham, and A. Vaishali, "Glossary of metaheuristic algorithms," *Int. J. Comput. Inf. Syst. Ind. Manage. Appl.*, vol. 9, pp. 181–205, Jun. 2017.
- [63] G. G. Wang, S. Deb, and Z. Cui, "Monarch butterfly optimization," *Neural Comput. Appl.*, vol. 31, no. 7, pp. 1995–2014, 2019.
- [64] G.-G. Wang, S. Deb, and L. D. S. Coelho, "Elephant herding optimization," in *Proc. 3rd Int. Symp. Comput. Bus. Intell. (ISCBI)*, Bali, Indonesia, Dec. 2015, pp. 7–9.
- [65] G.-G. Wang, "Moth search algorithm: A bio-inspired Metaheuristic algorithm for global optimization problems," *Memetic Comput.*, vol. 10, no. 2, pp. 151–164, Jun. 2018.
- [66] S. Li, H. Chen, M. Wang, A. A. Heidari, and S. Mirjalili, "Slime mould algorithm: A new method for stochastic optimization," *Future Gener. Comput. Syst.*, vol. 111, pp. 300–323, Oct. 2020.
- [67] A. A. Heidari, S. Mirjalili, H. Farris, I. Aljarah, M. Mafarja, and H. Chen, "Harris hawks optimization: Algorithm and applications," *Future Gener. Comput. Syst.*, vol. 97, pp. 849–872, Aug. 2019.
- [68] S. Mirjalili, S. M. Mirjalili, and A. Lewis, "Grey wolf optimizer," *Adv. Eng. Softw.*, vol. 69, pp. 46–61, Mar. 2014.
- [69] E. Rakhshani, I. M. H. Naveh, H. Mehrjerdi, and K. Pan, "An optimized LQG servo controller design using LQI tracker for VSP-based AC/DC interconnected systems," *Int. J. Electr. Power Energy Syst.*, vol. 129, Jul. 2021, Art. no. 106752.
- [70] D. Karaboga and B. Basturk, "On the performance of artificial bee colony (ABC) algorithm," *Appl. Soft Comput.*, vol. 8, no. 1, pp. 687–697, Jan. 2008.
- [71] X. He, W. Wang, J. Jiang, and L. Xu, "An improved artificial bee colony algorithm and its application to multi-objective optimal power flow," *Energies*, vol. 8, no. 4, pp. 2412–2437, Mar. 2015.
- [72] S.-J. Huang and X.-Z. Liu, "Application of artificial bee colony-based optimization for fault section estimation in power systems," *Int. J. Electr. Power Energy Syst.*, vol. 44, no. 1, pp. 210–218, Jan. 2013.
- [73] M. Dorigo, M. Birattari, and T. Stutzle, "Ant colony optimization," *IEEE Comput. Intell. Mag.*, vol. 1, no. 4, pp. 28–39, Nov. 2006.
- [74] M. Dorigo and G. D. Caro, "Ant colony optimization: A new meta-heuristic," in *Proc. Congr. Evol. Comput. (CEC)*, vol. 2, 1999, pp. 1470–1477.
- [75] J. Kennedy and R. Eberhart, "Particle swarm optimization," in *Proc. Int. Conf. Neural Netw. (ICNN)*, vol. 4, 1995, pp. 1942–1948.
- [76] I. C. Trelea, "The particle swarm optimization algorithm: Convergence analysis and parameter selection," *Inf. Process. Lett.*, vol. 85, no. 6, pp. 317–325, Mar. 2003.
- [77] J. B. Odili, M. N. M. Kahar, and S. Anwar, "African buffalo optimization: A swarm-intelligence technique," *Procedia Comput. Sci.*, vol. 76, pp. 443–448, Jan. 2015.
- [78] S. Mirjalili, "The ant lion optimizer," *Adv. Eng. Softw.*, vol. 83, pp. 80–98, May 2015.
- [79] X. Yang and A. H. Gandomi, "Bat algorithm: A novel approach for global engineering optimization," *Eng. Comput.*, vol. 29, no. 5, pp. 464–483, Jul. 2012.
- [80] D. T. Pham, A. Ghanbarzadeh, E. Koç, S. Otri, S. Rahim, and M. Zaidi, "The bees algorithm—A novel tool for complex optimisation problems," in *Intelligent Production Machines and Systems*, D. T. Pham, E. E. Eldukhri, and A. J. Soroka, Eds. Oxford, U.K.: Elsevier, 2006, pp. 454–459.
- [81] A. Ayes, "Beaver algorithm for network security and optimization: Preliminary report," in *Proc. IEEE Int. Conf. Syst., Man Cybern.*, Oct. 2009, pp. 3657–3662.
- [82] Y. Marinakis and M. Marinaki, "A bumble bees mating optimization algorithm for the open vehicle routing problem," *Swarm Evol. Comput.*, vol. 15, pp. 80–94, Apr. 2014.
- [83] D. Teodorovic and M. Dell'Orco, "Bee colony optimization—A cooperative learning approach to complex transportation problems," *Adv. OR AI Methods Transp.*, vol. 51, pp. 51–60, Sep. 2005.
- [84] B. Niu and H. Wang, "Bacterial colony optimization," *Discrete Dyn. Nature Soc.*, vol. 2012, Jan. 2012, Art. no. 698057.
- [85] X. Lu and Y. Zhou, "A novel global convergence algorithm: Bee collecting pollen algorithm," in *Advanced Intelligent Computing Theories and Applications With Aspects of Artificial Intelligence*. Berlin, Germany: Springer, 2008, pp. 518–525.
- [86] K. M. Passino, "Biomimicry of bacterial foraging for distributed optimization and control," *IEEE Control Syst. Mag.*, vol. 22, no. 3, pp. 52–67, Mar. 2002.
- [87] H. F. Wedde, M. Farooq, and Y. Zhang, "BeeHive: An efficient fault-tolerant routing algorithm inspired by honey bee behavior," in *Ant Colony Optimization and Swarm Intelligence*, M. Dorigo, M. Birattari, C. Blum, L. M. Gambardella, F. Mondada, T. Stützle, Eds. Berlin, Germany: Springer, 2004, pp. 83–94.
- [88] S. Bitam and A. Mellouk, "Bee life-based multi constraints multicast routing optimization for vehicular ad hoc networks," *J. Netw. Comput. Appl.*, vol. 36, no. 3, pp. 981–991, May 2013.
- [89] A. Askarzadeh and A. Rezaeizadeh, "A new heuristic optimization algorithm for modeling of proton exchange membrane fuel cell: Bird mating optimizer," *Int. J. Energy Res.*, vol. 37, no. 10, pp. 1196–1204, Aug. 2013, doi: 10.1002/er.2915.
- [90] T. Sato and M. Hagiwara, "Bee system: Finding solution by a concentrated search," *IEEJ Trans. Electron., Inf. Syst.*, vol. 118, no. 5, pp. 721–726, 1998.
- [91] R. Akbari, A. Mohammadi, and K. Ziarati, "A novel bee swarm optimization algorithm for numerical function optimization," *Commun. Nonlinear Sci. Numer. Simul.*, vol. 15, no. 10, pp. 3142–3155, Oct. 2010.
- [92] S.-C. Chu, P.-W. Tsai, and J.-S. Pan, "Cat swarm optimization," in *PRI-CAI 2006: Trends in Artificial Intelligence*. Berlin, Germany: Springer, 2006, pp. 854–858.
- [93] X.-S. Yang and S. Deb, "Cuckoo search via Lévy flights," in *Proc. World Congr. Nature Biologically Inspired Comput. (NaBIC)*, 2009, pp. 210–214.
- [94] X. Meng, Y. Liu, X. Gao, and H. Zhang, "A new bio-inspired algorithm: Chicken swarm optimization," in *Advances in Swarm Intelligence*. Cham, Switzerland: Springer, 2014, pp. 86–94.
- [95] S. Mirjalili, "Dragonfly algorithm: A new meta-heuristic optimization technique for solving single-objective, discrete, and multi-objective problems," *Neural Comput. Appl.*, vol. 27, no. 4, pp. 1053–1073, May 2016.
- [96] Y. Shiqin, J. Jianjun, and Y. Guangxing, "A dolphin partner optimization," in *Proc. WRI Global Congr. Intell. Syst.*, vol. 1, 2009, pp. 124–128.
- [97] X.-S. Yang, "Firefly algorithms for multimodal optimization," in *Stochastic Algorithms: Foundations and Applications*, Berlin, Germany: Springer, 2009, pp. 169–178.

- [98] B. Xing and W.-J. Gao, "Frog inspired algorithms," in *Innovative Computational Intelligence: A Rough Guide to 134 Clever Algorithms*, B. Xing and W.-J. Gao, Eds. Cham, Switzerland: Springer, 2014, pp. 157–165.
- [99] B. Xing and W.-J. Gao, "Fruit fly optimization algorithm," in *Innovative Computational Intelligence: A Rough Guide to 134 Clever Algorithms*, B. Xing and W.-J. Gao, Eds. Cham, Switzerland: Springer, 2014, pp. 167–170.
- [100] C. Yang, J. Chen, and X. Tu, "Algorithm of fast marriage in honey bees optimization and convergence analysis," in *Proc. IEEE Int. Conf. Autom. Logistics*, Aug. 2007, pp. 1794–1799.
- [101] X. L. Li, "An optimizing method based on autonomous animats: Fish-swarm algorithm," *Syst. Eng.-Theory Pract.*, vol. 22, no. 11, pp. 32–38, 2002.
- [102] C. J. A. B. Filho, F. B. de Lima Neto, A. J. C. C. Lins, A. I. S. Nascimento, and M. P. Lima, "A novel search algorithm based on fish school behavior," in *Proc. IEEE Int. Conf. Syst., Man Cybern.*, Oct. 2008, pp. 2646–2651.
- [103] H. Min and Z. Wang, "Group escape behavior of multiple mobile robot system by mimicking fish schools," in *Proc. IEEE Int. Conf. Robot. Biomimetics*, Dec. 2010, pp. 320–326.
- [104] K. N. Krishnanand and D. Ghose, "A glowworm swarm optimization based multi-robot system for signal source localization," in *Design and Control of Intelligent Robotic Systems*, D. Liu, L. Wang, and K. C. Tan, Eds. Berlin, Germany: Springer, 2009, pp. 49–68.
- [105] S. Nakrani and C. Tovey, "On honey bees and dynamic allocation in an Internet server colony," in *Proc. 2nd Int. Workshop Math. Algorithms Social Insects*, Atlanta, GA, USA, Dec. 2003, pp. 1–8.
- [106] D. Karaboga and B. Akay, "A survey: Algorithms simulating bee swarm intelligence," *Artif. Intell. Rev.*, vol. 31, nos. 1–4, pp. 61–85, Jun. 2009.
- [107] O. B. Haddad, A. Afshar, and M. A. Mariño, "Honey-bees mating optimization (HBMO) algorithm: A new heuristic approach for water resources optimization," *Water Resour. Manage.*, vol. 20, no. 5, pp. 661–680, Oct. 2006.
- [108] R. Oftadeh and M. J. Mahjoob, "A new meta-heuristic optimization algorithm: Hunting search," in *Proc. 5th Int. Conf. Soft Comput., Comput. Words Perceptions Syst. Anal., Decis. Control*, Sep. 2009, pp. 1–5.
- [109] A. H. Gandomi and A. H. Alavi, "Krill herd: A new bio-inspired optimization algorithm," *Commun. Nonlinear Sci. Numer. Simul.*, vol. 17, no. 12, pp. 4831–4845, Dec. 2012.
- [110] H. A. Abbass, "MBO: Marriage in honey bees optimization—A haplometrosis polygynous swarming approach," in *Proc. Congr. Evol. Comput.*, vol. 1, 2001, pp. 207–214.
- [111] S. Mirjalili, "Moth-flame optimization algorithm: A novel nature-inspired heuristic paradigm," *Knowl.-Based Syst.*, vol. 89, pp. 228–249, Nov. 2015.
- [112] Y. Zhu, X. Feng, and H. Yu, "Mosquito host-seeking algorithm based on random walk and game of life," in *Intelligent Computing Theories and Application*. Cham, Switzerland: Springer 2018, pp. 693–704.
- [113] E. Duman, M. Uysal, and A. F. Alkaya, "Migrating birds optimization: A new metaheuristic approach and its performance on quadratic assignment problem," *Inf. Sci.*, vol. 217, pp. 65–77, Dec. 2012.
- [114] T. C. Havens, C. J. Spain, N. G. Salmon, and J. M. Keller, "Roach infestation optimization," in *Proc. IEEE Swarm Intell. Symp.*, Sep. 2008, pp. 1–7.
- [115] M. M. Eusuff and K. E. Lansey, "Optimization of water distribution network design using the shuffled frog leaping algorithm," *J. Water Resour. Planning Manage.*, vol. 129, no. 3, pp. 210–225, May 2003.
- [116] M. Hersovici, M. Jacovi, Y. S. Maarek, D. Pelleg, M. Shtalhaim, and S. Ur, "The shark-search algorithm. An application: Tailored Web site mapping," *Comput. Netw. ISDN Syst.*, vol. 30, nos. 1–7, pp. 317–326, Apr. 1998.
- [117] C. Anandaraman, A. V. M. Sankar, and R. Natarajan, "A new evolutionary algorithm based on bacterial evolution and its application for scheduling a flexible manufacturing system," *Jurnal Teknik Industri*, vol. 14, no. 1, pp. 1–12, Jun. 2012.
- [118] R. Martin and W. Stephen, "Termite: A swarm intelligent routing algorithm for mobile wireless ad-hoc networks," in *Stigmergic Optimization*. Springer, 2006, pp. 155–184.
- [119] X.-S. Yang, "Engineering optimizations via nature-inspired virtual bee algorithms," in *Artificial Intelligence and Knowledge Engineering Applications: A Bioinspired Approach*. Berlin, Germany: Springer, 2005, pp. 317–323.
- [120] C. Liu, X. Yan, C. Liu, and H. Wu, "The wolf colony algorithm and its application," *Chin. J. Electron.*, vol. 20, no. 2, pp. 664–667, 2011.
- [121] S. Mirjalili and A. Lewis, "The whale optimization algorithm," *Adv. Eng. Softw.*, vol. 95, pp. 51–67, May 2016.
- [122] C. Yang, X. Tu, and J. Chen, "Algorithm of marriage in honey bees optimization based on the wolf pack search," in *Proc. Int. Conf. Intell. Pervas. Comput. (IPC)*, Oct. 2007, pp. 462–467.
- [123] P. C. Pinto, T. A. Runkler, and J. M. C. Sousa, "Wasp swarm algorithm for dynamic MAX-SAT problems," in *Adaptive and Natural Computing Algorithms*. Berlin, Germany: Springer, 2007, pp. 350–357.
- [124] Z. Feng, S. Liu, W. Niu, Z. Jiang, B. Luo, and S. Miao, "Multi-objective operation of cascade hydropower reservoirs using TOPSIS and gravitational search algorithm with opposition learning and mutation," *Water*, vol. 11, no. 10, p. 2040, Sep. 2019.
- [125] X. Yuan, B. Zhang, P. Wang, J. Liang, Y. Yuan, Y. Huang, and X. Lei, "Multi-objective optimal power flow based on improved strength Pareto evolutionary algorithm," *Energy*, vol. 122, pp. 70–82, Mar. 2017.
- [126] T. Bai, Y.-B. Kan, J.-X. Chang, Q. Huang, and F.-J. Chang, "Fusing feasible search space into PSO for multi-objective cascade reservoir optimization," *Appl. Soft Comput.*, vol. 51, pp. 328–340, Feb. 2017.
- [127] H. Tizhoosh, "Opposition-based learning: A new scheme for machine intelligence," in *Proc. Int. Conf. Comput. Intell. Modelling, Control Automat. Int. Conf. Intell. Agents, Web Technol. Internet Commerce*, Vienna, Austria, 2005, pp. 695–701.
- [128] S. Rahnamayan, H. R. Tizhoosh, and M. M. A. Salama, "Quasi-oppositional differential evolution," in *Proc. IEEE Congr. Evol. Comput.*, Sep. 2007, pp. 2229–2236.
- [129] C. Condordia, "Voltage stability of power systems: Concepts. Analytical tools and industry experience," IEEE/PES, Piscataway, NJ, USA, IEEE Tech. Rep. 90YH0358-2-PWR, 1990.
- [130] N. A. Wahab, M. R. Katebi, and J. Balderud, "Multivariable PID control design for wastewater systems," in *Proc. Medit. Conf. Control Autom.*, Jun. 2007, pp. 1–6.
- [131] E. Yeşil, M. Güzelkaya, and İ. Eksin, "Self tuning fuzzy PID type load and frequency controller," *Energy Convers. Manage.*, vol. 45, no. 3, pp. 377–390, Feb. 2004.
- [132] R. C. Dorf and R. H. Bishop, *Modern Control Systems*. Upper Saddle River, NJ, USA: Prentice-Hall, 2001.

• • •